International Journal of Pharmaceutics 414 (2011) 86–103

Contents lists available at ScienceDirect

International Journal of Pharmaceutics

journal homepage: www.elsevier.com/locate/ijpharm

Investigation of the riddle of sulfathiazole polymorphism

Mohd R. Abu Bakar[a,c], Zoltan K. Nagy[a,*], Chris D. Rielly[a], Sandy E. Dann[b]

[a] Department of Chemical Engineering, Loughborough University, Loughborough, Leicestershire, LE11 3TU, United Kingdom
[b] Department of Chemistry, Loughborough University, Loughborough, Leicestershire, LE11 3TU, United Kingdom
[c] Department of Pharmaceutical Technology, Kulliyyah of Pharmacy, International Islamic University Malaysia, Bandar Indera Mahkota, 25200 Kuantan, Pahang, Malaysia

ARTICLE INFO

Article history:
Received 12 January 2011
Received in revised form 28 April 2011
Accepted 2 May 2011
Available online 10 May 2011

Keywords:
Sulfathiazole
Process analytical technology
Solid state analysis

ABSTRACT

Since the discovery of sulfathiazole as an antimicrobial agent in 1939, numerous works in the screening for its different polymorphic forms, which is an essential part of drug development, have been conducted and published. These works consequently result in the availability of various methods for generating a particular polymorph. By following these methods, however, one cannot be guaranteed to obtain the intended pure polymorph because most of the methods do not clearly and adequately describe the crystallisation conditions, such as cooling rates and initial solute concentrations. In this paper, the available methods for generating all the known polymorphs of sulfathiazole are reviewed and selected methods for generating certain polymorphs, performed with their processes monitored using process analytical technology tools, i.e. focussed beam reflectance measurement and attenuated total reflectance ultraviolet spectroscopy, are presented. The properties of the obtained crystals, examined using various characterisation methods, are also presented and whenever possible, are compared with those of other workers.

1. Introduction

Sulfathiazole, a chemical structure shown in Fig. 1, is an antimicrobial agent. Since its discovery in 1939 (Fosbinder and Walter, 1939; Lott and Bergeim, 1939), numerous works in isolating, generating and characterising its different polymorphic forms have been carried out and communicated to the scientific community. True to a famous suggestion by Walter McCrone, that the number of polymorphic forms known for a given compound is proportional to the time and money spent in research on that compound (McCrone, 1965), the official knowledge on the number of sulfathiazole polymorphic forms has progressed from two in 1941 (Grove and Keenan, 1941) to five from 1999 (Hughes et al., 1999; Chan et al., 1999) until present. Sulfathiazole is also reported to form an amorphous phase (Mesley and Houghton, 1967; Lagas and Lerk, 1981), a hydrate (Kuhnert-Brandstätter and Wunsch, 1969) and over one hundred solvates (Bingham et al., 2001).

The extensive and repeated works on sulfathiazole polymorphism have produced inconsistent nomenclatures in the naming of the polymorphs. This inconsistency may cause confusion and difficulty in identifying and interpreting the literature information on the polymorphs and, as highlighted by Bernstein (2002), is due to the lack of attempts by authors to reconcile their own work with previous studies. Some authors, however, have corresponded and/or referred to their polymorphs using the notations of the Cambridge Structural Database (CSD) reference codes (refcodes) (Blagden et al., 1998; Aaltonen et al., 2003; Karjalainen et al., 2005; Hakkinen et al., 2005; Pollanen et al., 2005; Gelbrich et al., 2008; Alvarez et al., 2009). The refcodes can be considered as standards since each one of them represents specific crystallographic properties. There are currently 24 crystal structures of sulfathiazole available in the database to represent five different polymorphs. These structures are contributed by various researchers. A large number of structures to represent only five different polymorphs indicate that some of them are repeated. However, the later deposited data are expected to provide improved quality in their structural representations, particularly with respect to the hydrogen atom positions. This is due to the improved X-ray diffractometer's capability as a result of the technological advances. In order to differentiate between different polymorphs, the CSD also uses the enumeration scheme adopted by the earlier crystal structures' depositors. Table 1 relates the scheme to the corresponding refcodes. In this paper, the enumeration of the sulfathiazole polymorphs follows this scheme. Attempts to reconcile the literature enumeration of sulfathiazole polymorphs have been made by Burger and Dialer (1983) and Anwar et al. (1989). Here, their works were updated and extended to include all five known polymorphs as well as the un-cited and later literature. Table 1 also relates

* Corresponding author. Tel.: +44 01509 222 516; fax: +44 01509 223 953.
E-mail address: Z.K.Nagy@lboro.ac.uk (Z.K. Nagy).

0378-5173/$ – see front matter © 2011 Elsevier B.V. All rights reserved.
doi:10.1016/j.ijpharm.2011.05.004

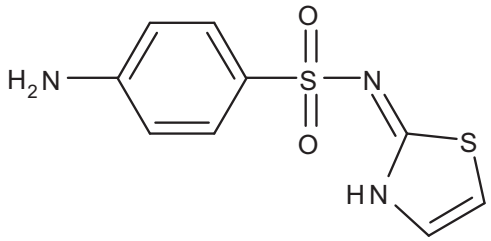

Fig. 1. Chemical structure of sulfathiazole.

the literature enumeration of the sulfathiazole polymorphs to the enumeration scheme and refcodes adopted by the CSD.

The numerous works on sulfathiazole polymorphism have also resulted in the availability of various methods for generating a particular polymorph. By following these methods, however, one cannot be guaranteed to obtain the intended pure polymorph because most of them do not clearly and adequately describe the crystallisation conditions, such as cooling rates and initial solute concentrations. It has been suggested that the failure to adequately describe the crystallisation conditions is one of the factors that led to the confusion over the identity of sulfathiazole polymorphs (Hughes et al., 1999). The implementation of process analytical technology (PAT), which involves the use of *in situ* analysers that are able to measure, monitor and record the process properties and the indication of product quality in real-time, is one of the strategies to fully describe the crystallisation conditions (Yu et al., 2003). This paper presents the work in generating sulfathiazole polymorphs using crystallisation methods that were selected from the literature. The crystallisations were performed with the processes monitored using focussed beam reflectance measurement (FBRM) and attenuated total reflectance ultraviolet spectroscopy (ATR-UV) spectroscopy. In order to assess the success of these polymorph crystallisations, the obtained crystals were examined using various characterisation techniques including optical microscopy, scanning electron microscopy (SEM), differential scanning calorimetry (DSC), thermogravimetry (TG), hot-stage microscopy (HSM), Fourier transform infrared (FT-IR) spectroscopy and X-ray powder diffractometry (XRPD) and whenever possible the results were compared with those of previous workers.

The works presented in this paper were undertaken with the following objectives: (a) to provide a comprehensive literature review on the crystallisation and polymorphism of sulfathiazole. This includes a compilation of literature methods for isolating a particular polymorph and a reconciliation of various enumerations of the polymorphs that are in use from 1941 to present; (b) to offer reliable methods of generating sulfathiazole polymorphs through *in situ* monitoring and thorough recording of process properties using FBRM and ATR-UV spectroscopy; and (c) to understand and differentiate sulfathiazole polymorphs properly – an essential prior knowledge in the design and development of a polymorphic control approach.

2. Crystallisation of sulfathiazole polymorphs

Since the polymorphism of sulfathiazole has been extensively and repeatedly investigated by various researchers as shown in Table 1, various recipes for generating a particular polymorph have become available.

Table 1
Literature enumeration of sulfathiazole polymorphs and the corresponding CSD enumeration and refcode.

CSD enumeration	Equivalent CSD refcode	Literature enumeration and reference
Form I	Suthaz01, Suthaz07, Suthaz08, Suthaz16, Suthaz23.	Rod form (Grove and Keenan, 1941); *β* (Miyazaki, 1947); *B* (Mesley and Houghton, 1967); *II* (Milosovich, 1964; Higuchi et al., 1967; Guillory, 1967; Moustafa and Carless, 1969; Shenouda, 1970; Shami et al., 1972; Carless and Jordan, 1974; Jordan and Carless, 1976); *I* (Lagas and Lerk, 1981; Anwar et al., 1989; Mesley, 1971; Kruger and Gafner, 1971, 1972; Gelbrich et al., 2008; Burger and Dialer, 1983; Shaktshneider and Boldyrev, 1993; Khoshkhoo and Anwar, 1993; Apperley et al., 1999; Luner et al., 2000; Blagden et al., 1998; Zeitler et al., 2006; Parmar et al., 2007; Drebushchak et al., 2008).
Form II	Suthaz, Suthaz03, Suthaz09, Suthaz10, Suthaz18, Suthaz20.	Hexagonal form (Grove and Keenan, 1941); *α* (Miyazaki, 1947); *A* (Mesley and Houghton, 1967); *I* (Shami et al., 1972); *II′* (Babilev et al., 1987); *II* (Blagden et al., 1998; Kruger and Gafner, 1971, 1972; Blagden, 2001; Parmar et al., 2007; Drebushchak et al., 2008); *IV* (Anwar et al., 1989; Burger and Dialer, 1983; Khoshkhoo and Anwar, 1993; Apperley et al., 1999; Zeitler et al., 2006; Gelbrich et al., 2008).
Form III	Suthaz02, Suthaz11, Suthaz12, Suthaz17, Suthaz21.	*α′* (Miyazaki, 1947); *C* (Mesley and Houghton, 1967); *IIA* (Mesley, 1971); *I* (Milosovich, 1964; Higuchi et al., 1967; Guillory, 1967; Moustafa and Carless, 1969; Shenouda, 1970; Carless and Jordan, 1974; Jordan and Carless, 1976); *III* (Lagas and Lerk, 1981; Blagden et al., 1998; Anwar et al., 1989; Kruger and Gafner, 1971, 1972; Gelbrich et al., 2008; Burger and Dialer, 1983; Shaktshneider and Boldyrev, 1993; Khoshkhoo and Anwar, 1993; Apperley et al., 1999; Luner et al., 2000; Blagden, 2001; Zeitler et al., 2006; Parmar et al., 2007; Drebushchak et al., 2008; Ali et al., 2009).
Form IV	Suthaz04, Suthaz13, Suthaz14, Suthaz19, Suthaz22.	*IIB* (Mesley, 1971); *II* (Khoshkhoo and Anwar, 1993); *IV* (Blagden et al., 1998; Babilev et al., 1987; Blagden, 2001; Parmar et al., 2007; Drebushchak et al., 2008); *V* (Apperley et al., 1999; Zeitler et al., 2006; Gelbrich et al., 2008).
Form V	Suthaz05, Suthaz06, Suthaz15.	*V* (Hughes et al., 1999; Chan et al., 1999); *II* (Lagas and Lerk, 1981; Anwar et al., 1989; Burger and Dialer, 1983; Apperley et al., 1999; Zeitler et al., 2006; Gelbrich et al., 2008).

Table 2
Methods of producing Form I.

No.	Procedure	Reference
1	Seeded cooling crystallisation from a saturated n-propanol solution at 80–90 °C. After a crop of rod-like crystals has formed, the hot supernatant solvent was decanted and drained off. The crystals were washed with ether to remove solvent and then dried in the air at room temperature.	Grove and Keenan (1941) and Higuchi et al. (1967)
2	Cooling crystallisation from a saturated n-propanol solution at 80–90 °C.	Mesley and Houghton (1967), Shenouda (1970), Kruger and Gafner (1971, 1972), Lagas and Lerk (1981), Burger and Dialer (1983), Anwar et al. (1989), Khoshkhoo and Anwar (1993), Blagden et al. (1998), Blagden (2001), Karjalainen et al. (2005) and Parmar et al. (2007)
3	Cooling crystallisation from a saturated solution of amyl alcohol.	Miyazaki (1947) and Moustafa and Carless (1969)
4	Cooling crystallisation from a saturated solution of isobutanol.	Miyazaki (1947) and Mesley and Houghton (1967)
5	Cooling crystallisation from a saturated solution of n-butanol at its boiling temperature.	Shaktshneider and Boldyrev (1993), Parmar et al. (2007) and Drebushchak et al. (2008).
6	Cooling crystallisation from a saturated solution of *sec*-butanol.	Higuchi et al. (1967), Moustafa and Carless (1969) and Shenouda (1970)
7	Heating a commercial raw material or Form II or Form III at a temperature between 170 and 180 °C for 15–40 min.	Miyazaki (1947), Milosovich (1964), Moustafa and Carless (1969), Shami et al. (1972), Carless and Jordan (1974), Shaktshneider and Boldyrev (1993), Apperley et al. (1999), Luner et al. (2000) and Zeitler et al. (2006)

2.1. Form I

Literature recipes for isolating Form I are presented in Table 2. It can be seen from the table that all of the solvents that have been used to crystallise Form I are alcohols containing between three to five carbon atoms, which satisfy a suggestion made by Mesley (1971) that recrystallisations from alcohols containing three or more carbon atoms should produce Form I. In accordance to the Ostwald's Rule of Stages, Blagden et al. (1998) suggested that any solvent should be able to initially produce Form I as it is the least stable form, followed by a stepwise conversion, through the other metastable forms, to the thermodynamically most stable form. An example of this stepwise conversion had been observed by Grove and Keenan (1941) during their attempt to isolate rod-like Form I crystals from hot ethanol. In order to prevent any polymorphic conversions, n-propanol was chosen as the solvent since it has a higher boiling point than ethanol, which they reckoned will allow enough time for the crystals to be removed from the hot solution before the conversion can take place; hence the origin of Method 1. However, it was reported much later that Form I crystallised from n-propanol did not transform to other forms up to one year of storage as slurry at 30 °C (Blagden et al., 1998).

All of the cited researchers that utilised Method 1 and Method 2 in Table 2 implied no presence of any other polymorphic forms besides Form I, but more recent researchers reported otherwise. Anderson et al. (2001) reported that although crystallisations from n-propanol at various cooling rates in stirred and unstirred 50 mL reactors consistently produced Form I, traces of Form V were also found within some samples. The crystals obtained by Aaltonen et al. (2003) through cooling crystallisation from n-propanol at a constant rate of 35 °C/h in a 100 mL reactor were mainly Form I, but Form II and Form III were also present. Through a cooling crystallisation experiment conducted at a constant rate of 27.5 °C/h in a 4 L reactor, Hakkinen et al. (2005) obtained crystals of mainly Form I together with some portions of Form III and Form V. More recently, Alvarez et al. (2009) produced Form I, Form III and Form IV from cooling crystallisation experiments using n-propanol as a solvent at various initial concentrations and cooling rates.

Method 7 in Table 2 was first applied by Miyazaki (1947). The method can be considered as the most reliable one because at the heating temperature, crystals of Form II, or Form III, or the commercial raw material, which is typically composed of Form II or Form III, or a mixture of the two, are expected to transform into Form I since it is the most stable sulfathiazole polymorph at high temperature. Although the heating process may turn the crystals into a

Table 3
Methods of producing Form II.

No.	Procedure	Reference
1	Cooling crystallisation from a saturated n-propanol solution at room temperature.	Kruger and Gafner (1971, 1972) and Burger and Dialer (1983)
2	Cooling crystallisation from water to room temperature.	Grove and Keenan (1941) and Miyazaki (1947)
3	Cooling crystallisation from a saturated acetone solution to room temperature.	Grove and Keenan (1941) and Miyazaki (1947)
4	Cooling crystallisation from a mixture of acetone and chloroform. A saturated acetone solution was cooled to room temperature and diluted with chloroform.* A 1:1* or 3:2† mixture of acetone:chloroform was used.	Mesley and Houghton (1967), Shami et al. (1972), Anwar et al. (1989)* and Khoshkhoo and Anwar (1993)†
5	Slow† cooling crystallisation from a saturated ethanol solution to room temperature. Store in the slurry for a month at 30 °C*.	Grove and Keenan (1941), Miyazaki (1947), Babilev et al. (1987)† and Blagden et al. (1998)*
6	Cooling a saturated solution of sulfathiazole in nitromethane (26 g/L) to 30 °C and store in the slurry for a month at that temperature.	Blagden et al. (1998)
7	Cooling crystallisation from a saturated methanol solution to room temperature.	Grove and Keenan (1941), Miyazaki (1947) and Parmar et al. (2007)
8	Cooling crystallisation from a saturated acetonitrile solution.	Apperley et al. (1999) and Zeitler et al. (2006)
9	Slow concentrating a solution in a methanol–acetonitrile mixture.	Drebushchak et al. (2008)

Table 4
Methods of producing Form III.

No.	Procedure	Reference
1	Dissolving in a cold dilute ammonium hydroxide solution, followed by warming up the solution surface to obtain the crystals.	Miyazaki (1947)
2	Slow evaporation of a diluted ammonium hydroxide solution at room temperature.	Kruger and Gafner (1971) and Shaktshneider and Boldyrev (1993)
3	Cooling crystallisation from a dilute ammonium hydroxide solution (1% or 10% or 20%). Store in the slurry for a month at 30 °C.	Mesley and Houghton (1967), Moustafa and Carless (1969), Shenouda (1970) and Blagden et al. (1998)
4	Slow crystallisation from warm ethanol.	Milosovich (1964), Higuchi et al. (1967), Shenouda (1970) and Lagas and Lerk (1981)
5	Evaporation of methanol solution.	Mesley and Houghton (1967)
6	Cooling crystallisation from water (cooling rate of 5–10 °C/h).	Moustafa and Carless (1969), Mesley (1971), Jordan and Carless (1976), Lagas and Lerk (1981), Anwar et al. (1989), Khoshkhoo and Anwar (1993) and Karjalainen et al. (2005).
7	Cooling crystallisation from a mixture of acetone–chloroform (3:1).	Moustafa and Carless (1969), Shenouda (1970) and Lagas and Lerk (1981)
8	Cooling crystallisation from a mixture of benzene:ethanol (3:1).	Shenouda (1970)
9	Cooling crystallisation from isopropanol.	Shenouda (1970), Luner et al. (2000) and Parmar et al. (2007)
10	Slow cooling crystallisation from aqueous ethanol (95% or 40%).	Moustafa and Carless (1969), Carless and Jordan (1974), Lagas and Lerk (1981) and Burger and Dialer (1983)
11	Replacement of acetone by dichloromethane in boiling solution.	Apperley et al. (1999)
12	Slow evaporating of a solution of ethanol–water–ammonia mixture.	Drebushchak et al. (2008).

slight off-white colour, it was found that this did not interfere with the subsequent characterisation studies (Apperley et al., 1999).

2.2. Form II

Table 3 summarizes methods of producing Form II. Although Method 1 was the method used by the researchers that contributed the crystallographic data for Form II (Kruger and Gafner, 1971); it is not a reliable method to produce Form II crystals based on a recent work by Alvarez et al. (2009), which showed that cooling crystallisation experiments from initial temperature of 30 °C produced only Form III at a slow cooling rate and no crystals at all when a fast cooling rate was applied. In addition, as mentioned previously, only a small portion of Form II was obtained by Aaltonen et al. (2003) through their cooling crystallisation experiment from n-propanol at a constant rate of 35 °C/h. Based on the same set of works by Alvarez et al. (2009), Method 2 is also not a reliable method of producing Form II because only Form III and Form IV were obtained in their cooling crystallisation experiments with water as the solvent (Alvarez et al., 2009). On the same note, Blagden et al. (1998) also reported that crystallisation from water only favours the formation of Form IV crystals. Although Form II was produced by cooling crystallisation experiments from both acetone and a mixture of acetone and chloroform, as reported by Alvarez et al. (2009), it always formed as a mixture with Form III. On the other hand, based on a report by Mesley (1971), recrystallisation from a mixture of acetone and chloroform did not produce Form II at all, but a mixture of Form III and Form IV. For these reasons, Method 3 and Method 4 are not reliable methods of generating Form II crystals. Method 5 was the method used by Babilev et al. (1987), the contributor of the crystallographic data of Suthaz03 (Form II). Slightly over a decade later, Blagden et al. (1998) also used the same method to produce Form II crystals in their study on the effect of solvent to the polymorph appearance. In the same study, they also generated Form II crystals from nitromethane (Method 6). Method 7, Method 8 and Method 9 are also believed to be reliable since Parmar, Apperley, Drebushchak and their co-workers were able to produce crystals with X-ray diffraction parameters consistent with literature values of Form II.

2.3. Form III

Methods of producing Form III are presented in Table 4. Method 1, Method 2 and Method 3 involve fast evaporation, slow evaporation and cooling crystallisation, respectively, using the same solvent, i.e. a diluted ammonium hydroxide. Method 2 was used by Kruger and Gafner (1971) in their work, which the crystallographic data of Form III originated. Method 4 is basically similar to one of the reliable methods of producing Form II (Method 5 in Table 3); therefore its reliability to generate Form III at the same time is suspicious. Method 5 uses the same solvent as another reliable method of producing Form II (Method 7 in Table 3) and although their mode of supersaturation generation is different – evaporation for Method 5 and cooling for the other; the method is still suspect since in determining the formation of a particular polymorph, the effect of solvent often dominates the effect of supersaturation (Khoshkhoo

Table 5
Methods of producing Form IV.

No.	Procedure	Reference
1	Cooling a saturated solution of sulfathiazole in water. Store in the slurry for a month at 30 °C.	Babilev et al. (1987), Blagden et al. (1998) and Parmar et al. (2007).
2	Rapid quenching a boiling solution of sulfathiazole in water to 4 °C.	Khoshkhoo and Anwar (1993)
3	Cooling crystallisation from aqueous ethanol.	Drebushchak et al. (2008).

Table 6
Methods of producing Form V.

No.	Procedure	Reference
1	Boiling a supersatured solution of sulfathiazole in water to dryness. As soon as the water evaporated, crystals are immediately dried in a hot air oven at 105 °C for 15 min.	Lagas and Lerk (1981), Anwar et al. (1989), Khoshkhoo and Anwar (1993), Hughes et al. (1999), Chan et al. (1999), Apperley et al. (1999), Anderson et al. (2001) and Zeitler et al. (2006).
2	Dissolving in n-propanol at 97 °C and cooled very slowly without rotation or agitation.	Burger and Dialer (1983)

and Anwar, 1993). Method 6 is also a suspicious method because it was reported that crystallisations from water produced either a mixture of Form III and Form IV (Alvarez et al., 2009) or Form IV (Blagden et al., 1998). Crystallisation from a mixture of acetone and chloroform, as mentioned earlier, always favour the formation of a mixture of polymorphs; either Form II and Form III (Alvarez et al., 2009) or Form III and Form IV (Mesley, 1971). For this reason, Method 7 is not a reliable method of producing Form III. The reliability of Method 8, first implemented by Shenouda (1970), has never been verified by later researchers. In that work, the obtained crystals were made to undergo inconclusive solid-state characterisation analyses, which subject the outcome of the application of the method to speculation. Method 9 was used by Parmar et al. (2007) to produce Form III and they found that the X-ray diffraction parameters of the obtained crystals match well to the literature values of the intended polymorph. The same method was also applied by Luner et al. (2000), who found that the measured density of the obtained crystals corresponded very well to the literature value of Form III. Method 10 and Method 11 were used by Burger and Dialer (1983) and Apperley et al. (1999), respectively. The methods are believed to be reliable since they have successfully differentiated different polymorphs they generated using a combination of solid-state characterisation techniques. Drebushchak et al. (2008) showed that the crystals they obtained using Method 12 gave X-ray diffraction parameters that are consistent with the literature values for Form III. This verifies the reliability of Method 12 to produce Form III.

2.4. Form IV

There are three methods of producing Form IV as shown in Table 5. Method 1 and Method 2 are basically the same in that both use water as the solvent; only Method 2 is clearer in describing the crystallisation conditions. Based on the work by Alvarez et al. (2009), cooling crystallisations from saturated water solutions at 90 °C with both fast (5 °C/min) and slow (1 °C/min) cooling rates consistently produced Form IV crystals. These findings proved the reliability of Method 2. Babilev et al. (1987) used Method 1 to come up with the crystallographic data for Form IV. Two decades later, Parmar et al. (2007) confirmed the repeatability of the same method to produce Form IV by showing that the crystals they obtained using Method 1 gave X-ray diffraction parameters that are consistent with the values given by Babilev et al. Drebushchak et al. (2008) were also able to produce crystals that give x-ray diffraction data similar to those given by Babilev et al.; in this case, however, the crystals were produced using Method 3. Although Method 3 in Table 5 may appear to be similar to Method 10 in Table 4, but it should be noted that different compositions of ethanol:water ratio have to be considered as different solvents.

2.5. Form V

As shown in Table 6, most of researchers used Method 1 to generate Form V; most notably among them are Hughes, Chan and their co-workers, who are the contributors of the crystallographic data for Form V and Form V, respectively. In order to ensure a successful outcome of the execution of Method 1, the transfer of the crystals to the hot air oven after the water has just evaporated must be quick enough; otherwise Form III will be formed instead (Anwar et al., 1989). The immediate transfer also prevents overheating of the crystals, which may turn them brown or decompose them. Method 2 is not a reliable method to produce Form V since n-propanol is a solvent known to favour the crystallisation of Form I or at least the crystals of mainly Form I. With the exception of Hakkinen et al.

Table 7
Methods of characterising sulfathiazole polymorphs.

No.	Method
1.	Density measurement: Flotation (Kruger and Gafner, 1971); Pyknometry (Burger and Dialer, 1983).
2.	Refractive indices (Grove and Keenan, 1941; Miyazaki, 1947).
3.	Solubility measurement (Lagas and Lerk, 1981; Milosovich, 1964; Burger and Dialer, 1983; Khoshkhoo and Anwar, 1993).
4.	Microscopy: Optical (Grove and Keenan, 1941; Blagden et al., 1998; Miyazaki, 1947; Parmar et al., 2007); Scanning electron (Hakkinen et al., 2005; Parmar et al., 2007).
5.	Thermal analysis: DSC (Lagas and Lerk, 1981; Anwar et al., 1989; Mesley, 1971; Anderson et al., 2001; Moustafa and Carless, 1969; Shenouda, 1970; Burger and Dialer, 1983; Shaktshneider and Boldyrev, 1993; Luner et al., 2000; Zeitler et al., 2006; Parmar et al., 2007; Ali et al., 2009); TG (Lagas and Lerk, 1981); HSM (Grove and Keenan, 1941; Anwar et al., 1989; Milosovich, 1964; Higuchi et al., 1967; Guillory, 1967; Shenouda, 1970; Burger and Dialer, 1983; Zeitler et al., 2006).
6.	Spectroscopy: IR (Mesley and Houghton, 1967; Lagas and Lerk, 1981; Anwar et al., 1989; Mesley, 1971; Anderson et al., 2001; Moustafa and Carless, 1969; Burger and Dialer, 1983; Shaktshneider and Boldyrev, 1993; Parmar et al., 2007); NIR (Aaltonen et al., 2003; Luner et al., 2000; Ali et al., 2009); Raman (Anwar et al., 1989; Anderson et al., 2001; Zeitler et al., 2006; Ali et al., 2009); Terahertz pulsed (Zeitler et al., 2006).
7.	NMR (Anwar et al., 1989; Apperley et al., 1999).
8.	X-ray diffraction: Powder (Chan et al., 1999; Anwar et al., 1989; Mesley, 1971; Aaltonen et al., 2003; Hakkinen et al., 2005; Kruger and Gafner, 1971; Higuchi et al., 1967; Shaktshneider and Boldyrev, 1993; Parmar et al., 2007; Ali et al., 2009); Single crystal (Hughes et al., 1999; Anwar et al., 1989; Kruger and Gafner, 1971; 1972; Babilev et al., 1987; Parmar et al., 2007); Variable temperature powder (Lagas and Lerk, 1981; Karjalainen et al., 2005); Variable temperature single crystal (Drebushchak et al., 2008).

Table 8
Summary of literature calculated density, melting temperature and polymorphic transformation from one form to another that is stable at high temperature.

Polymorph	Calculated density (g/cm^3)	Melting temperature (°C)	Transformation temperature into Form I (°C)
I	1.499 (Kruger and Gafner, 1972)	200–202 (Lagas and Lerk, 1981; Anwar et al., 1989; Mesley, 1971; Anderson et al., 2001; Zeitler et al., 2006)	–
II	1.550 (Kruger and Gafner, 1971)	173–175 (Grove & Keenan, 1941; Anwar et al., 1989; Apperley et al., 1999)	150–170 (Anwar et al., 1989); 138 (Zeitler et al., 2006)
III	1.567 (Kruger and Gafner, 1971)	173 (Miyazaki, 1947; Anwar et al., 1989; Lagas and Lerk, 1981; Shenouda, 1970; Moustafa and Carless, 1969)	105–170 (Lagas and Lerk, 1981);
		175 (Apperley et al., 1999)	150–170 (Anwar et al., 1989); 159 (Zeitler et al., 2006)
IV	1.595 (Babilev et al., 1987)	179 (Shenouda, 1970); 175 (Apperley et al., 1999)	160 (Zeitler et al., 2006)
V	1.510 (Hughes et al., 1999)	196–197 (Lagas and Lerk, 1981; Anwar et al., 1989; Anderson et al., 2001)	When Form V melts it immediately recrystallises into Form I (Lagas and Lerk, 1981)

(2005), who detected the presence of a small portion of Form V together with Form I and Form III, no other researchers reported the formation of Form V from n-propanol.

3. Solid-state characterisation of sulfathiazole polymorphs

Numerous characterisation methods, which vary from traditional to advanced instrumentations, have been utilised to examine and differentiate between different sulfathiazole polymorphs. The methods and the corresponding literature are presented in Table 7. Results of some of these solid-state characterisation studies are referred and compared accordingly with the present work.

Table 8 shows literature calculated density values for each of the sulfathiazole polymorphs. The values were obtained from the unit cell dimensions and mass. Since the most stable structure corresponds to the one with the most efficient packing, which in turn corresponds to the structure with the highest density, the density values can be used to rank the relative stability of the polymorphs. Based on the values; the ranking of the stability of the sulfathiazole polymorphs at ambient conditions is in the order of Form IV > Form III > Form II > Form V > Form I. The melting and transformation temperatures obtained from the literature, as shown in Table 8, indicate that at high temperature, Form I is the most stable polymorph since all other forms transformed to Form I above 105 °C.

4. Experimental

4.1. Materials

Sulfathiazole was purchased from Sigma–Aldrich with a purity of 98%. Based on the results of XRPD analysis, the received sulfathiazole is a mixture of Form III, Form IV and the amorphous form. The solvents used are *sec*-butanol, acetonitrile, isopropanol and deionized water. Except water, all other solvents were analytical reagent grade purchased from Fisher Scientific.

4.2. Solubility measurements

The solubilities of sulfathiazole in the respective solvents were determined at temperatures ranging from 25 °C to 70 °C using isothermal method (Myerson, 2002).

4.3. Crystallisation of sulfathiazole polymorphs

Different polymorphs were generated using the methods shown in Table 9. Methods 1–4, which utilised unseeded cooling crystallisations, were performed in a jacketed 500 mL glass vessel. The temperature in the vessel was controlled with a PTFE sheathed thermocouple connected to a thermo fluid circulator bath (Huber Variostat CC-415 vpc). The temperature readings were recorded every 20 s on a computer by a control interface written in LabVIEW (National Instruments). An overhead stirrer with a PTFE four pitch-bladed turbine was used to agitate the system between 220 and 320 rpm. The agitation speed was reduced to 150 rpm after nucleation in order to minimize damage to the crystals. An FBRM probe (model D600, Lasentec) was inserted into the solution to measure chord length distributions. The distributions were collected every 20 s and averaged during collection. They were monitored using the FBRM control interface software (version 6.7). The UV system used was a Zeiss MCS621 spectrometer with a CLD600 lamp module. Absorbance spectra were obtained through a Hellma 661.822 Attenuated Total Reflectance (ATR) UV/vis probe, which was directly immersed in the solution. The spectral range was 242–360 nm, and a spectrum of the solution was recorded every 20 s using a data acquisition software, Aspect Plus (version 1.76).

Table 9
Methods to produce different polymorphs of sulfathiazole.

Method no.	Polymorph to be produced	Procedure
1.	Form I	Based on Method 6, Table 2. A saturated solution at 70 °C was prepared by heating 2.4 g of sulfathiazole in 300 g of *sec*-butanol in a 0.5 L double jacketed crystalliser to dissolution, followed by natural cooling to 20 °C.
2.	Form II	Based on Method 8, Table 3. A saturated solution at 60 °C was prepared by heating 6.0 g of sulfathiazole in 240 g of acetonitrile in a 0.5 L double jacketed crystalliser to dissolution, followed by natural cooling to 20 °C.
3.	Form III	Based on Method 9, Table 4. A saturated solution at 70 °C was prepared by heating 3.0 g of sulfathiazole in 240 g of isopropanol in a 0.5 L double jacketed crystalliser to dissolution, followed by natural cooling to 25 °C.
4.	Form IV	Based on Method 2, Table 5. A saturated aqueous solution of sulfathiazole at 80 °C (3.0 g in 300 g water) was cooled rapidly to 4 °C at a set rate of 10 °C/min in a 0.5 L double jacketed crystalliser.
5.	Form V	Based on Method 1, Table 6. A saturated aqueous solution of sulfathiazole (4.0 g in 200 g water) was boiled to evaporate in a beaker on a hot plate until almost dry.

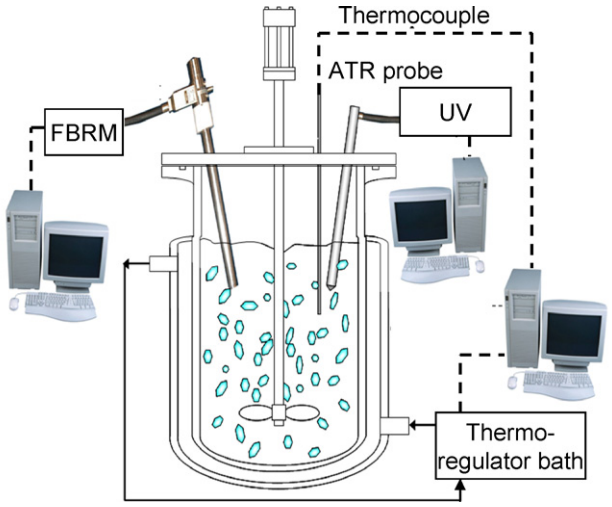

Fig. 2. A schematic representation of the experimental set-up.

A schematic representation of the experimental set-up is shown in Fig. 2. Method 5, which involved evaporative crystallisation, was performed in a 250 mL glass beaker on a Stuart CB162 heat-stir plate (Bibby Sterlin Ltd.). At the end of the crystallisation runs, the crystallised solids were vacuum filtered and subsequently, those crystals obtained from water, were immediately dried in a hot air oven at 105 °C for 15 min, whereas crystals obtained from other solvents were dried in a desiccator.

4.4. Characterisation of sulfathiazole polymorphs

Optical microscopy – the morphology of the crystals was observed using a Leica DMLM microscope. The captured microscopic images were analysed using Leica QWin (Leica Microsystems Digital Imaging).

SEM – samples were sparsely sprinkled onto carbon tape attached to metal stubs before thinly being coated with gold. The samples were then imaged using an SEM (Cambridge Streoscan 360) fitted with an Inca X-Sight (Oxford Instruments) detector. An accelerating voltage of 10 kV was used during imaging.

DSC – the thermal behaviour of the polymorphs was examined using a TA Instruments DSC Q10. About 8 mg of sample was weigh into an aluminium pan and sealed hermetically. Analysis was carried out by heating the sample from 100 to 240 °C at a heating rate of 10 °C/min under constant purging of nitrogen at 40 mL/min. An empty aluminium pan was used as a reference in all the runs. Results were analysed using TA Instruments Universal Analysis 2000.

TG – a PerkinElmer Pyris 1 TGA system was used for the TG analysis of the polymorphs. The analysis was conducted by heating the sample with a weight range of 2–10 mg from 25 °C to 200 °C at a constant heating rate of 10 °C/min.

HSM – the thermal behaviour of the polymorphs was visually examined using a Mettler Toledo FP90 hot-stage system and a Leica DMLM microscope with a 10× objective lens from 100 to 250 °C at a heating rate of 10 °C/min. Microscopic observations during experiments were displayed on a computer screen and recorded using a JVC colour video camera.

FT-IR spectroscopy – FT-IR spectra of the polymorphs were acquired using a Shimadzu FT-IR-8400S system at room temperature (approximately 25 °C). Spectra over a range of 4000–600 cm^{-1} with a resolution of 2 cm^{-1} were recorded using potassium bromide (KBr) discs. The discs were prepared earlier by mixing approximately 2 mg of sample in 300 mg of KBr (IR spectroscopy grade purchased from Fisher Scientific) and grinding them together using pestle and mortar. The resulting powder mixture was then pressed into disc using a laboratory hydraulic press.

XRPD – the XRD data were collected on powdered samples using a Bruker D8 X-ray powder diffractometer. The instrument used monochromated CuKα_1 radiation and a position sensitive detector (PSD). Samples were mounted in Perspex flat plate sample holders and analysed through a 2θ range of 5–35° using a step size of 0.014767° over a period of 60 min at a constant temperature of 25 °C. Theoretical diffraction patterns generated using the ATOMS 5.0 programme from the crystallographic data of each polymorph obtained from the CSD are used as reference data.

Table 10
Van't Hoff equations for sulfathiazole in various solvents.

Solvent	Van't Hoff equation
sec-Butanol	$C = 3.52 \times 10^5 e^{-4479/T}$
Acetonitrile	$C = 1.03 \times 10^5 e^{-3503/T}$
Isopropanol	$C = 0.68 \times 10^5 e^{-3845/T}$
Water	$C = 16.58 \times 10^5 e^{-5185/T}$

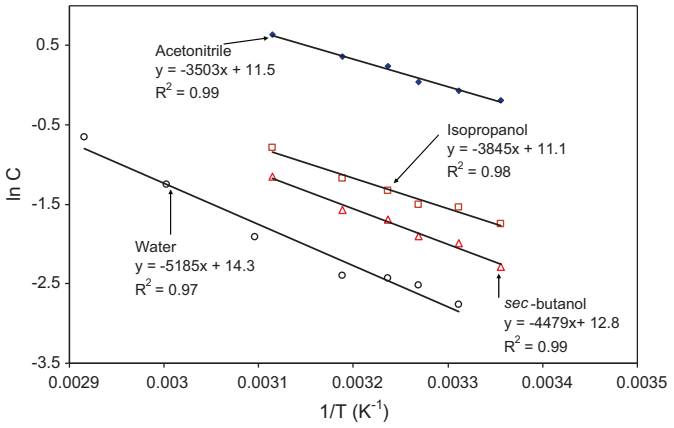

Fig. 3. Linearised van't Hoff solubility curves for sulfathiazole in *sec*-butanol, acetonitrile, isopropanol and water.

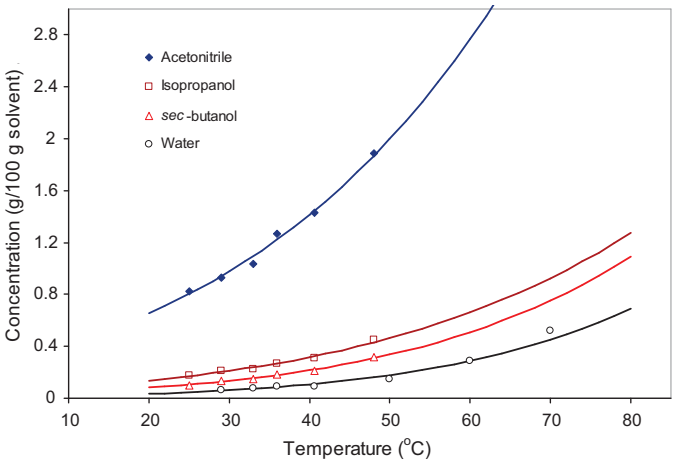

Fig. 4. Experimental solubility points (shown as markers) and the corresponding van't Hoff solubility curves for sulfathiazole in *sec*-butanol, acetonitrile, isopropanol and water. Solid lines represent van't Hoff solubility curves.

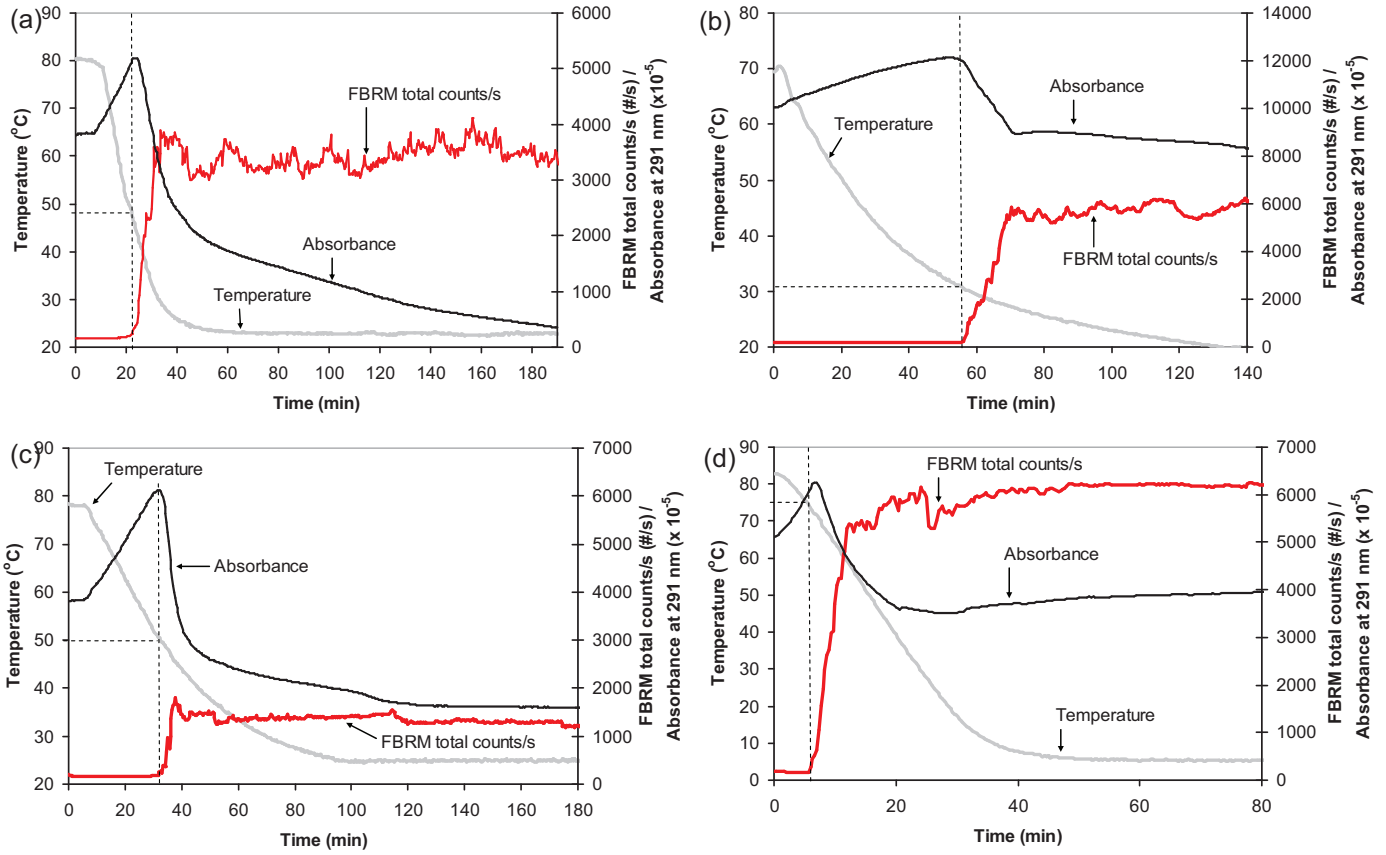

Fig. 5. Profiles of temperature, FBRM total number of counts/s and UV absorbance at 291 nm during cooling crystallisations for (a) Method 1; (b) Method 2; (c) Method 3, and (d) Method 4.

5. Results and discussion

5.1. Solubility measurements

The obtained solubility data for sulfathiazole in *sec*-butanol, acetonitrile, isopropanol and water were used to construct linearised van't Hoff solubility curves, as presented in Fig. 3. Linear regression analysis of the curves gave *R*-squared values between 0.97 and 0.99, which indicates the consistency and reliability of the experimental solubility data.

Based on van't Hoff equation, a plot of $\ln C$ against $1/T$ should give a straight line with a slope of $(-\Delta H_f/R)$ and an intercept of $(\Delta H_f/RT_f)$, where C is the concentration of the solute in the solution, ΔH_f is the molar enthalpy of fusion of the solute, R is the gas constant, T_f is the fusion temperature of the solute (K) and T is the solution temperature (K). For simplicity, the slope and intercept are now referred to as a and b, respectively. Rearrangement of the equation gives:

$$C = e^{b} \times e^{a/T} \quad (1)$$

The coefficients of the best-fit linear equations of the curves in Fig. 3 were substituted into Eq. (1) to relate concentration to absolute temperature as presented in Table 10.

Based on the equations in Table 10, van't Hoff solubility curves were plotted along with the experimental solubility points, as shown in Fig. 4. It can be inferred from the position of the solubility curves in the figure that the relative solubility of sulfathiazole in the selected solvents is in the order of acetonitrile > isopropanol > *sec*-butanol > water. The solubility values of sulfathiazole in *sec*-butanol and water at 30 °C were reported by Higuchi et al. (1967) as 0.149 g/100 g and 0.114 g/100 g, respectively. The values obtained in this work, however, are found to be 0.134 g/100 g and 0.061 g/100 g, respectively. Although deviates by almost 87% from Higuchi et al.'s, the solubility of sulfathiazole in water at 30 °C obtained in this work agrees well with the one extracted from the solubility curve given by Khoshkhoo and Anwar (1993), i.e. 0.066 g/100 g. The discrepancy between the solubility data is probably due to the difference in polymorphic form of the crystals. Based on the extensive literature review, this is the first time the solubility data for sulfathiazole in acetonitrile and isopropanol have been reported.

5.2. Crystallisation of sulfathiazole polymorphs

UV absorbance spectra at the highest peak, 291 nm, as marked by a dashed line in Appendix A, were used directly to qualitatively indicate the change of sulfathiazole concentration during the crystallisation processes, with the assumption that the absorbance is directly proportional to the concentration. Although the absorbance is also affected by the temperature; however, very often the impact can be differentiated easily from those of the nucleation, dissolution and polymorphic transformation events, which are normally characterised by the sudden change in the absorbance. The ATR-UV spectroscopy has been used quantitatively for the *in situ* monitoring and detection of nucleation event (Billot et al., 2010; Abu Bakar et al., 2009; Simon et al., 2009; Nagy et al., 2007; Anderson et al., 2001), as well as the polymorphic transformation (Howard et al., 2009; Nagy et al., 2007; Gillon et al., 2006).

The profiles of temperature, FBRM total number of counts/s and UV absorbance at 291 nm for cooling crystallisations performed in Method 1, Method 2, Method 3 and Method 4 are shown in Fig. 5. The temperature profile of the natural cooling was pre-

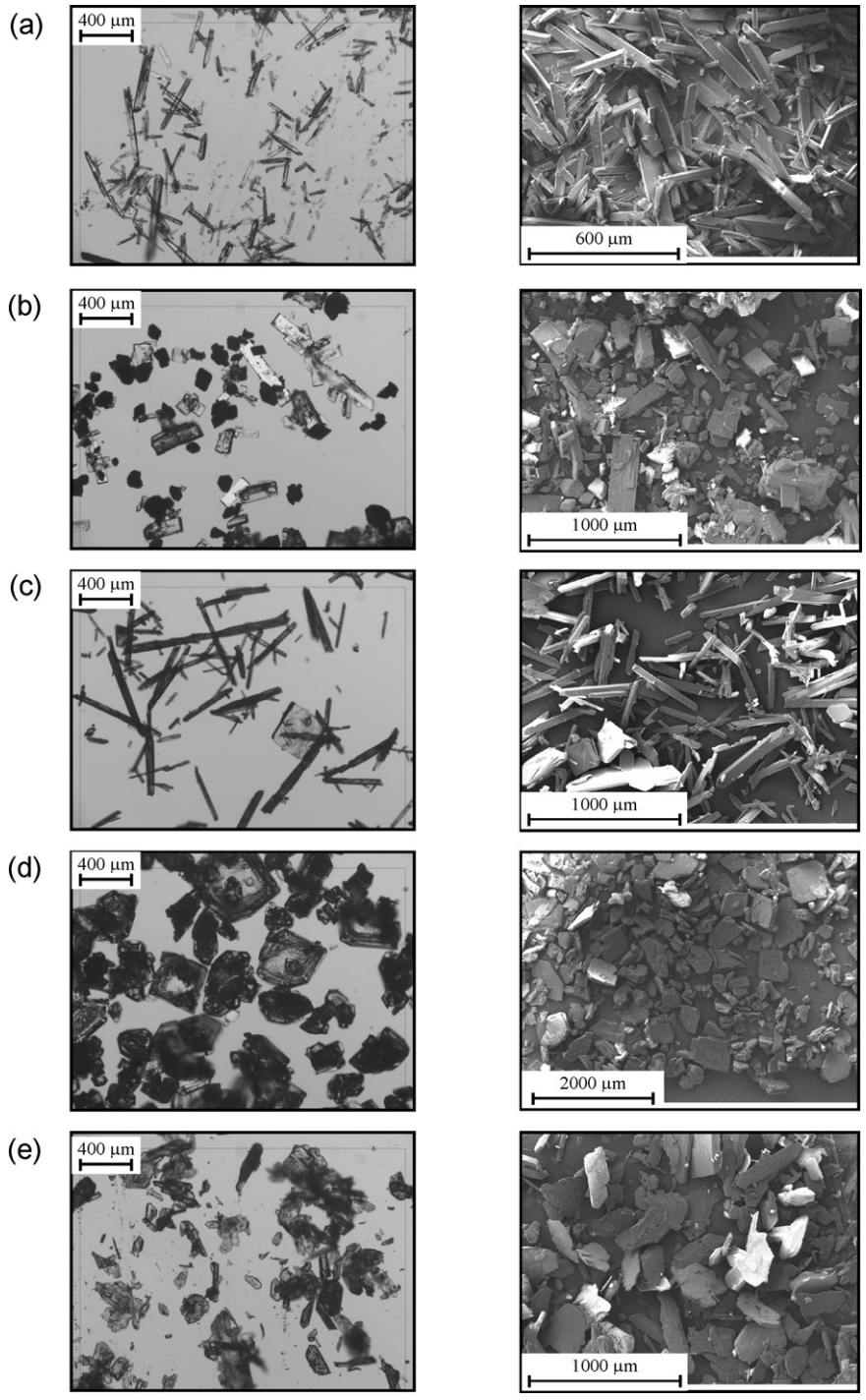

Fig. 6. Optical microscopy and SEM images of crystals obtained from (a) Method 1; (b) Method 2; (c) Method 3; (d) Method 4; and (e) Method 5.

determined from the actual natural cooling experiment performed in a 250 mL conical flask from 80 °C to ambient temperature, which was 25 °C. As can be observed in Fig. 5(a) for Method 1, when the system reached approximately 48 °C upon cooling, the FBRM total number of counts/s showed a sudden increase while the absorbance showed a sudden drop, which indicates the occurrence of nucleation event. Since the solution was prepared to be saturated at 70 °C, the metastable zone width (MSZW) of the system was calculated to be 22 °C. Once the number of counts/s eventually stabilized at approximately 3500 counts/s, the absorbance continued to drop slowly. This indicates that the growth dominated process has taken over the nucleation dominated phase of the process. A similar trend was also shown by the crystallisation processes for Method 2, Method 3 and Method 4 as can be seen in Fig. 5(b), (c) and (d), respectively. In these cases, the nucleation events were detected at approximately 31 °C for Method 2, 50 °C for Method 3, and 75 °C for Method 4 which gave the MSZWs of 29 °C, 20 °C and 15 °C, respectively. It can also be observed that prior to all the nucleation events, the absorbance was increasing on cooling, which is due to the effect of temperature change. In a solution at constant concentration, the absorbance generally increases with decreasing temperature. Hence for quantitative

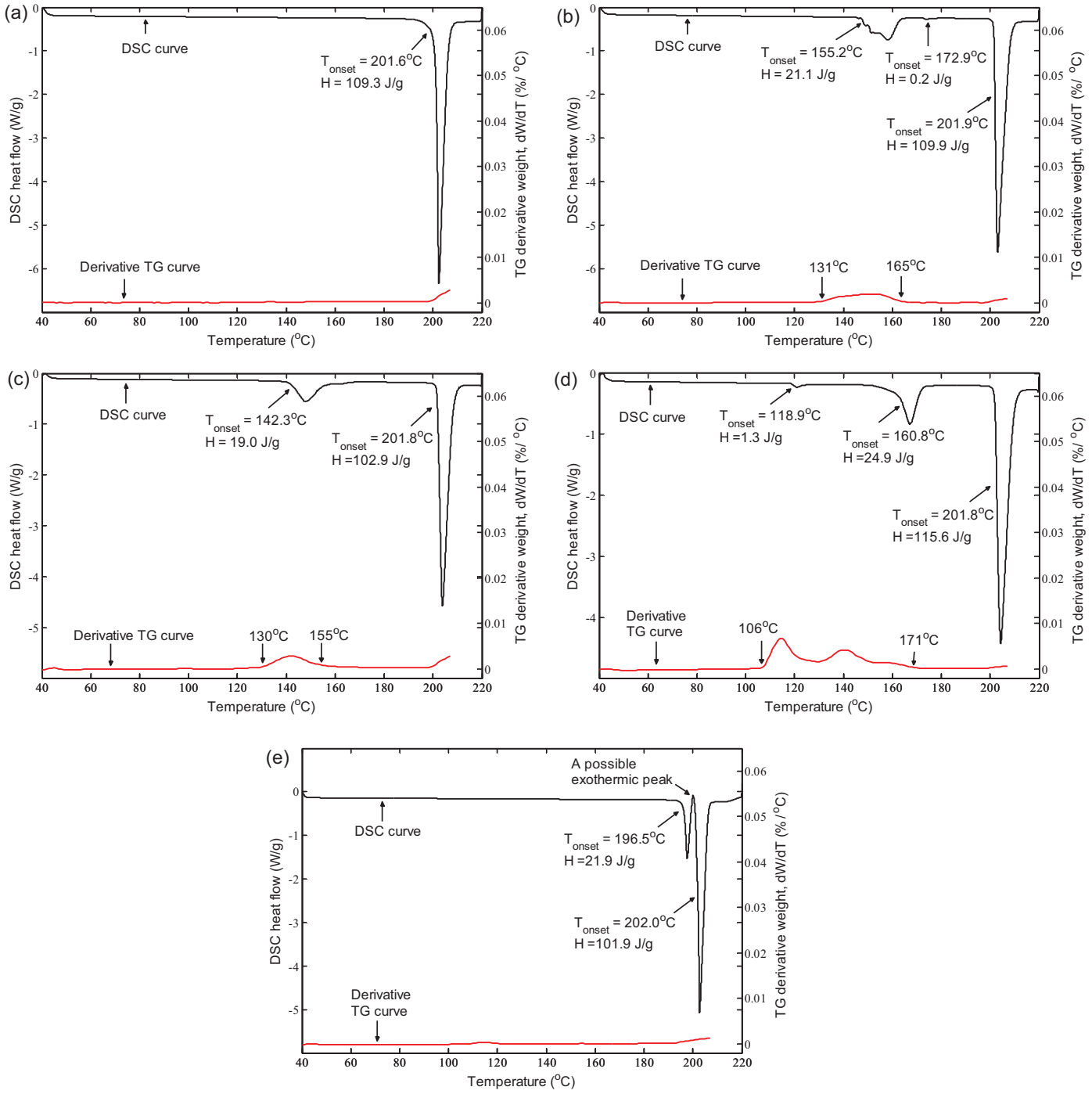

Fig. 7. DSC and derivative TG curves of crystals obtained by (a) Method 1; (b) Method 2; (c) Method 3; (d) Method 4, and (e) Method 5.

concentration measurement, the temperature effect has to be taken into account in the calibration as described in the previous work (Abu Bakar et al., 2009).

In addition to the provision of the clear and adequate initial crystallisation conditions, such as solute concentrations and temperatures, the *in situ* monitoring and thorough recording of the process properties in real-time would define the design range of the process parameters (temperature, FBRM total number of counts/s and UV absorbance) that has been demonstrated to provide the required crystal quality. By operating within this design range, the crystals can be reproduced with the same desired quality.

5.3. Characterisation of sulfathiazole polymorphs

5.3.1. Optical microscopy and SEM

Fig. 6 shows the optical microscopy and SEM images of crystals produced by (a) Method 1; (b) Method 2; (c) Method 3; (d) Method 4; and (e) Method 5. Based on the images given by these two microscopy techniques, the morphology of the crystals can be accurately described. It was found that the crystals that were recrystallised from *sec*-butanol (Method 1), as shown in Fig. 6(a), have a rod-like structure with an average length of approximately 400 μm. Form I crystals are normally reported to exhibit

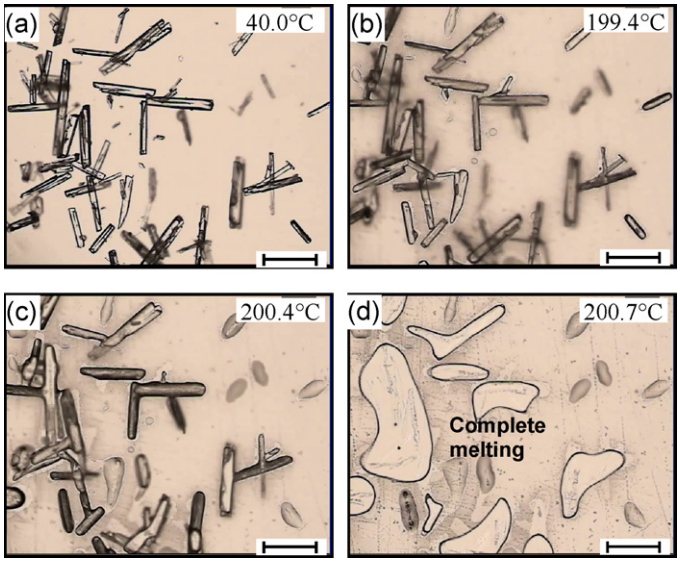

Fig. 8. Images of crystals obtained by Method 1 during HSM analysis taken at (a) 40.0 °C; (b) 199.4 °C; (c) 200.4 °C; and (d) 200.7 °C. The scale bars represent 200 μm.

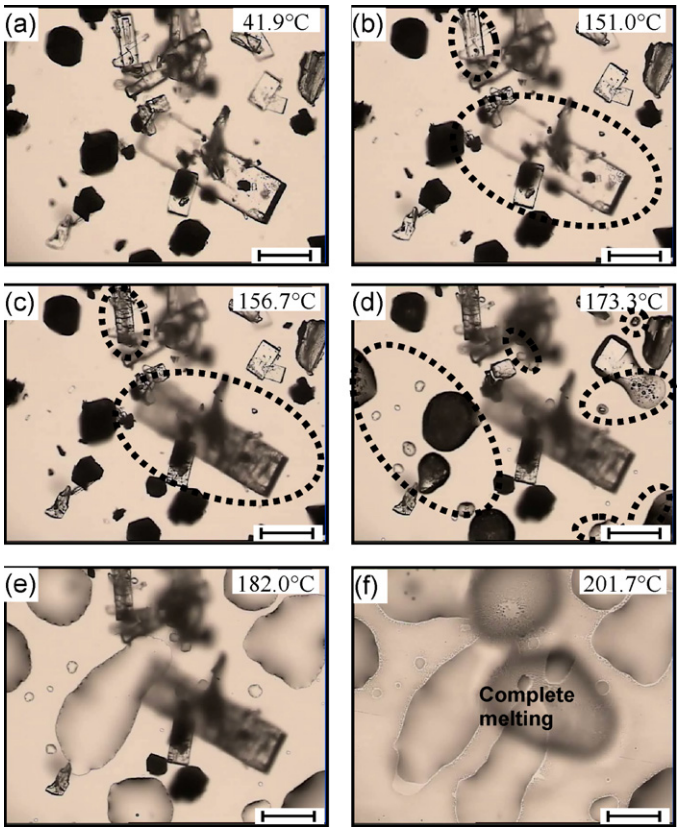

Fig. 9. Images of crystals obtained by Method 2 during HSM analysis taken at (a) 41.9 °C; (b) 151.0 °C; (c) 156.7 °C; (d) 173.3 °C; (e) 182.0 °C; and (f) 201.7 °C. The scale bars represent 200 μm.

this morphology regardless of the crystallizing solvent (Blagden et al., 1998; Parmar et al., 2007). This, according to Blagden and co-workers, implies that the available solvent–surface interactions cannot inhibit the growth of the fastest growing {0 1 0} faces. The crystals produced by Method 2, in which acetonitrile was the crystallizing solvent, were found to exhibit a mixture of morphology: rectangular plates and truncated rectangular rods as can be seen in Fig. 6(b). Images in Fig. 6(c) show that the crystals produced from isopropanol (Method 3) generally have a rod-like morphology, although the presence of square plate crystals was also observed. According to the work of Parmar et al. (2007), sulfathiazole initially crystallised from isopropanol as needles and very small square plates. The square plates then grew in size and the needles vanished. They also reported that the rate of crystal growth was slow and this may explain the appearance of the crystals produced in this work, which is mostly rod-like since the crystals were suspended in the crystallising solvent for only about 150 min. The morphology of the crystals obtained from water by fast cooling crystallisation (Method 4), shown in Fig. 6(d), can be categorized as a mixture of square and hexagonal plates. This is consistent with that reported in the literature for Form IV crystals (Blagden et al., 1998). On the other hand, the crystals obtained from water by evaporative crystallisation (Method 5), with their images presented in Fig. 6(e), were found to be irregular-shaped plates. Since the morphology of crystals depends very much on the crystallising solvent, as well as other factors including the degree of supersaturation and the state of agitation of the crystallisation system, morphology is not normally used to differentiate between polymorphs.

5.3.2. DSC, TG and HSM

The curves of the DSC and TG, and some snapshots during HSM analysis of the crystals obtained by Method 1 are presented in Fig. 7(a) and Fig. 8, respectively. The DSC curve shows one endothermic peak with an onset temperature of 201.6 ± 0.4 °C and a latent heat of 109.3 ± 5.9 J/g. It is widely known that Form I is the most stable sulfathiazole polymorph at high temperature and for the heating at 10 °C/min, it was reported to melt at a temperature between 200 °C and 202 °C (Lagas and Lerk, 1981; Anwar et al., 1989; Mesley, 1971; Anderson et al., 2001; Zeitler et al., 2006) and released a latent heat of fusion between 81.8 J/g and 108.5 J/g (Lagas and Lerk, 1981; Zeitler et al., 2006). Although a melting event should not be detected by TG, however, as can be observed from Fig. 7(a), the obtained derivative TG curve shows a very small weight change at approximately the same temperature as the melting peak on the DSC curve. This is probably due to the loss of trapped solvent or sublimation of sample during the melting process. The HSM analysis was found to agree very well with the results of the DSC and TG analyses. As shown by the snapshots of the crystals during the HSM analysis in Fig. 8(c), most of the crystals started to melt when the hot-stage temperature reached 200.4 °C. A complete melting of the crystals was observed slightly above 200.7 °C, as can be seen in Fig. 8(d). The absence of other thermal events prior to the melting of Form I, as shown by all three thermal analysis methods, indicates that Method 1 is a reliable method to produce pure Form I crystals.

The DSC and derivative TG curves of the crystals obtained by Method 2 are shown in Fig. 7(b), while some snapshots of the crystals during HSM analysis are presented in Fig. 9. The DSC curve shows the presence of two major and one minor endothermic peaks. The first major peak at an onset temperature of 155.2 ± 0.6 °C and a latent heat of 21.1 ± 2.1 J/g was contributed by the change in the optical properties of the crystals, as shown by the difference in the brightness of the highlighted crystals between (b) and (c) in Fig. 9, which can be associated with a solid-solid transformation event. It was reported that a transformation from one polymorph to another could be accompanied by a striking change in birefringence (Miller and Sommer, 1966). The temperature of the presumed transformation event observed in this work is consistent with a previous report. Anwar et al. (1989) reported that Form II crystals may transform into Form I in a temperature range of 150–170 °C. Zeitler et al. (2006), on the other hand, reported a slightly lower transformation temperature, i.e. 138 °C and a higher heat of transformation, i.e. 32.4 J/g. The derivative TG curve in Fig. 7(b) shows an increase in the rate of weight change between 131 °C and 165 °C,

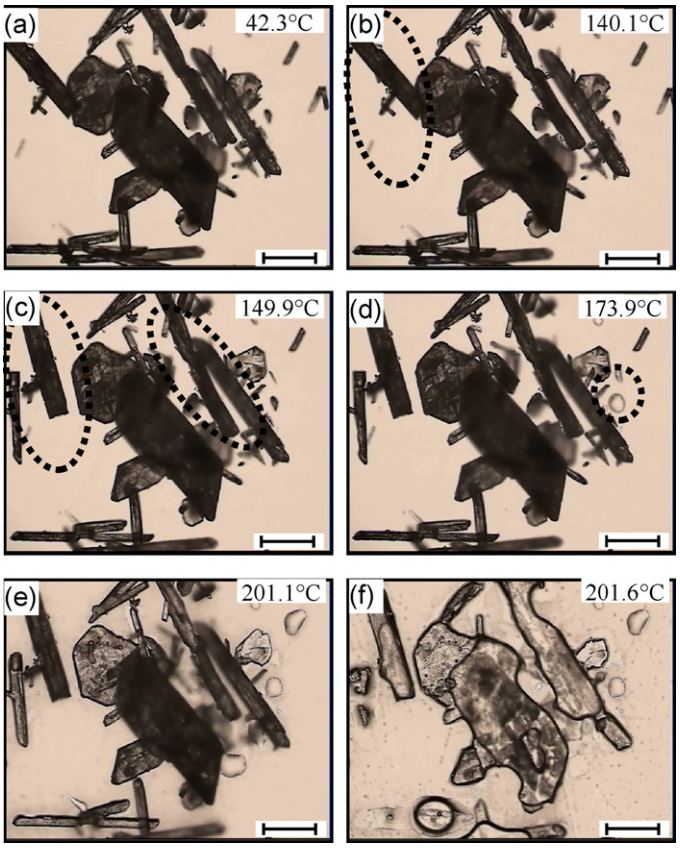

Fig. 10. Images of crystals obtained by Method 3 during HSM analysis taken at (a) 42.3 °C; (b) 140.1 °C; (c) 149.9 °C; (d) 173.9 °C; (e) 201.1 °C; and (f) 201.6 °C. The scale bars represent 200 μm.

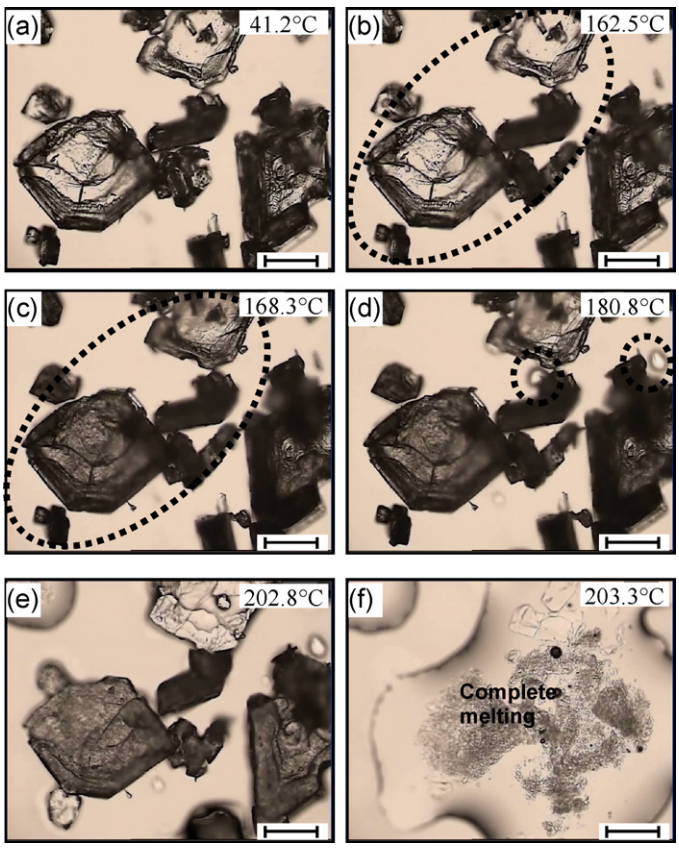

Fig. 11. Images of crystals obtained by Method 4 during HSM analysis taken at (a) 41.2 °C; (b) 162.5 °C; (c) 168.3 °C; (d) 180.8 °C; (e) 202.8 °C; and (f) 203.3 °C. The scale bars represent 200 μm.

which is almost in the same vicinity as the first DSC peak. Since the calculated mole fraction of the solvent presents in the sample is very small, i.e. 0.0035; there is no reason to suppose that the crystals are solvates. The change in the weight was believed to be due to a polymorphic transformation. The transformation involves rearrangement of the crystal structures and in doing so may remove some volatile impurities that are trapped in the structures. The snapshots of the crystals during the HSM analysis in Fig. 9(d) and (e) show that all crystals, except those that had undergone optical property change, melted between 173.3 °C and 182.0 °C. This event, however, only registered as a minor endothermic peak at 172.9 °C with a latent heat of 0.2 J/g on the DSC curve, which suggests that only small quantity of crystals were involved. The melting of Form II at a temperature between 173 °C and 175 °C has been reported by previous researchers (Grove & Keenan, 1941; Anwar et al., 1989). The melting of the remaining crystals at 201.7 °C, as shown by the HSM analysis in Fig. 9(f), is consistent with the second major peak on the DSC curve, which lies at an onset of 201.9 ± 0.0 °C with a latent heat of 109.9 ± 1.7 J/g. The results of the DSC, TG and HSM analyses imply that some of the crystals obtained by Method 2 have transformed to Form I in a temperature range of 155.2–165 °C. Those crystals that were not transformed melted at a temperature between 172.9 °C and 173.3 °C, while the newly formed Form I crystals melted at a temperature between 201.7 °C and 201.9 °C. This is actually one of the two reasonable explanations suggested by Anwar et al. (1989), who also observed similar behaviour exhibited by sulfathiazole crystals other than Form I and Form V. Another explanation is that two polymorphs were initially formed; one melted at a temperature between 172.9 °C and 173.3 °C and another transformed to Form I in a temperature range of 155.2–165 °C.

The DSC curve of the crystals obtained by Method 3 presented in Fig. 7(c) demonstrates the presence of two endothermic peaks. The first peak with an onset temperature of 142.3 ± 0.4 °C and a latent heat of 19.0 ± 1.9 J/g was contributed by a possible polymorphic transformation, which was indicated by a slight movement of some of the crystals during HSM analysis as shown by the highlighted crystals in Fig. 10(b) and (c). Besides an optical property change,

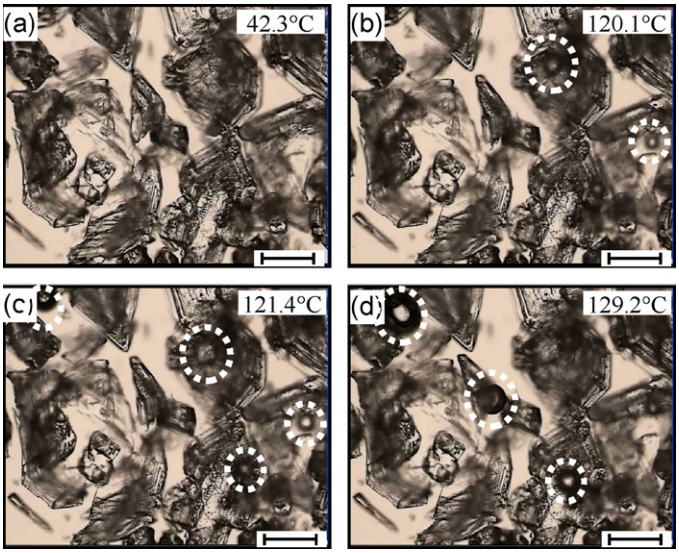

Fig. 12. Images of crystals obtained by Method 4 immersed in silicon oil during HSM analysis taken at (a) 42.3 °C; (b) 120.1 °C; (c) 121.4 °C; and (d) 129.2 °C. The scale bars represent 200 μm.

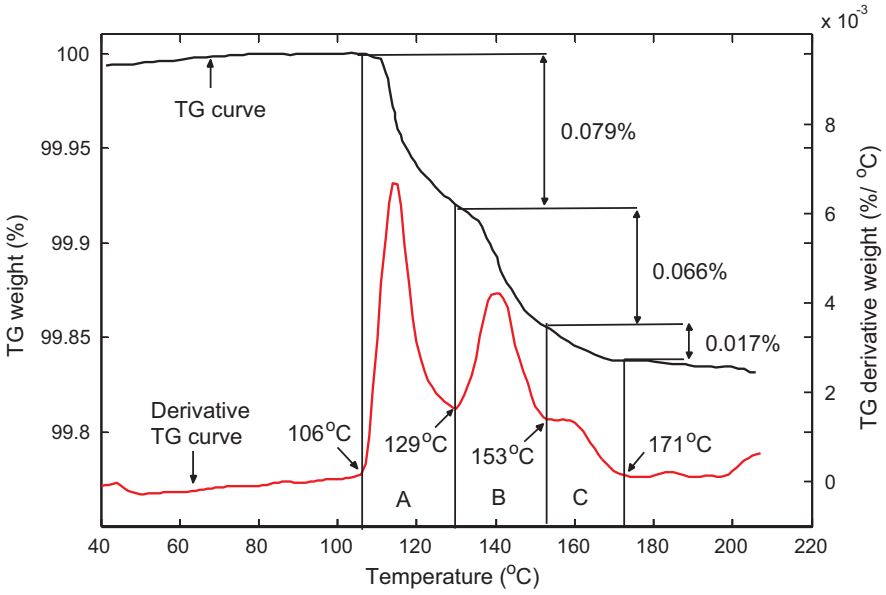

Fig. 13. TG and derivative TG curves of crystals obtained by Method 4.

a polymorphic transformation may also result in a movement of the crystals since the transformation events may be accompanied by a change in the crystals' volume (Warrington, 2002). The temperature of the transformation event observed in this work lies within the 105–170 °C range, in which Form III crystals may transform into Form I, as reported by Lagas and Lerk (1981), but outside the 150–170 °C range reported by Anwar et al. (1989). Zeitler et al. (2006) also reported a higher transformation temperature, i.e. 159 °C and a higher heat of transformation, i.e. 27.3 J/g. The derivative TG curve in Fig. 7(c) indicates an increase in the rate of weight change between 130 °C and 155 °C. The increase corresponds well with the endothermic peak that is associated with the polymorphic transformation. The mole fraction of the solvent presents in the sample was calculated to be 0.0023; too small to consider the crystals as solvates. The second peak on the DSC curve has an onset temperature of 201.8 ± 0.1 °C and a latent heat of 102.9 ± 7.5 J/g was the result of the melting of Form I crystals. The melting was confirmed by the HSM analysis, as shown in Fig. 10(f), Although the HSM analysis showed the melting of a few tiny crystal fragments at 173.9 °C, as highlighted in Fig. 10(d), the DSC curve does not show any melting peak in the vicinity of that temperature, due to either a negligible impact of the event on the overall thermal process or a complete absence of the melting species in the DSC samples. However, both results are consistent with the reports by the previous researchers (Miyazaki, 1947; Anwar et al., 1989; Lagas and Lerk, 1981; Shenouda, 1970; Moustafa and Carless, 1969) about the behaviour of Form III crystals during thermal analysis, which were summarized by Anwar et al. (1989) as either melted at 173 °C, or transformed to Form I between 150 °C and 170 °C before melting at 201 °C, or showed a combined behaviour. The single melting at 173 °C was postulated to be obtained only if the crystals are purely Form III (Lagas and Lerk, 1981). If the slightest amount of Form I was present, some, if not all Form III crystals will transform to Form I. Since Form I is expected to always be initially crystallised in accordance to the Ostwald's Rule of Stages, the likelihood of the contamination of the crystallisation product with Form I is very high. In general, the results of the DSC, TG and HSM indicate that Method 3 was able to produce Form III crystals. If the suggestion by the previous researchers about the effect of the presence of Form I on the transformation of Form III is true, then Method 3 also produced Form I crystals along with Form III crystals. The presence or absence of Form I crystals can be confirmed by the XRPD analysis, as shown later.

The results of the DSC and TG analyses of the crystals obtained using Method 4 are presented in Fig. 7(d). Three endothermic peaks are shown by the DSC curve. The first peak was formed at an onset of 118.9 ± 0.0 °C, the second at 160.8 ± 2.3 °C and the third at 201.8 ± 0.2 °C. Their enthalpies are 1.3 ± 0.6 J/g, 24.9 ± 0.9 J/g and 115.6 ± 4.2 J/g, respectively. The HSM analysis, however, only confirmed the last two events as shown by the snapshots of the crystals during the HSM analysis in Fig. 11. A polymorphic transformation was detected at 168.3 °C based on the optical property change of the highlighted crystals in Fig. 11(b) and (c). This is consistent with the second peak on the DSC curve. The transformation of Form IV crystals to Form I was also detected by Zeitler et al. (2006) at almost the same onset temperature, i.e. 160 °C, but it produced a slightly higher heat, i.e. 29.5 J/g. The HSM detected a melting event at 180.8 °C, as shown by the highlighted crystal fragments in Fig. 11(d). This event may be too small to be detected by the DSC, or the melting species was not present in the DSC samples. The temperature of the melting was slightly higher than those found previously (in crystals obtained by Method 2 and Method 3), but Shenouda (1970) have also reported melting events at 179 °C, given by the DSC analysis. Form IV, as well as Form II and Form III, have been reported to melt in the vicinity of 175 °C (Apperley et al., 1999). The melting of Form I crystals was shown by the HSM at 203.3 °C as depicted in Fig. 11(f). This is consistent with the third peak on the DSC curve. In contrast to the result of the DSC analysis, no thermal event was detected by the HSM in the vicinity of 118.9 °C. It was reported recently that the DSC peak that lies in the vicinity of that temperature corresponds to the dehydration of a hydrate (Howard et al., 2009). In order to confirm the presence of hydrates, the crystals were heated while immersed in silicone oil. Some of the images during the analysis were presented in Fig. 12. It was found that some bubbles were liberated at 120.1 °C, as highlighted in Fig. 12(b). The evolution and movement of these bubbles were seen in the subsequent snapshots in (c) and (d) in Fig. 12. This liberation of bubbles is believed to correspond to the escape of water vapor during the vaporization process, which would never be visually detected without the use of oil.

The derivative TG curve as shown in Fig. 7(d) indicates the removal of volatile impurities between 106 °C and 171 °C, which

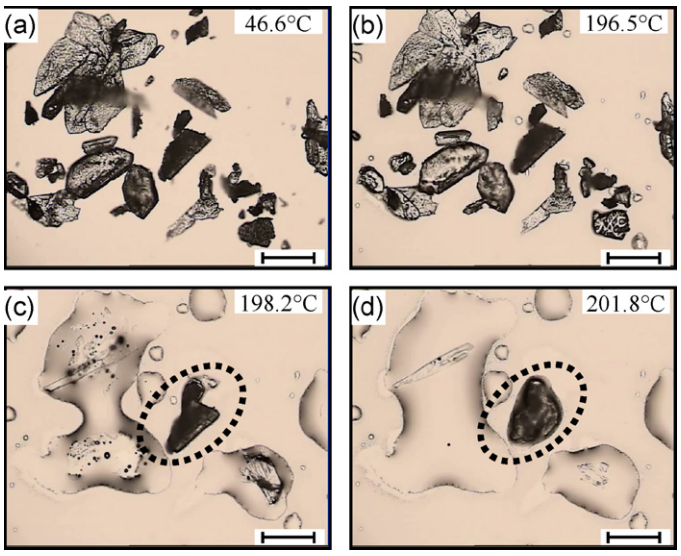

Fig. 14. Images of crystals obtained by Method 5 during HSM analysis taken at (a) 46.6 °C; (b) 196.5 °C; (c) 198.2 °C; and (d) 201.8 °C. The scale bars represent 200 μm.

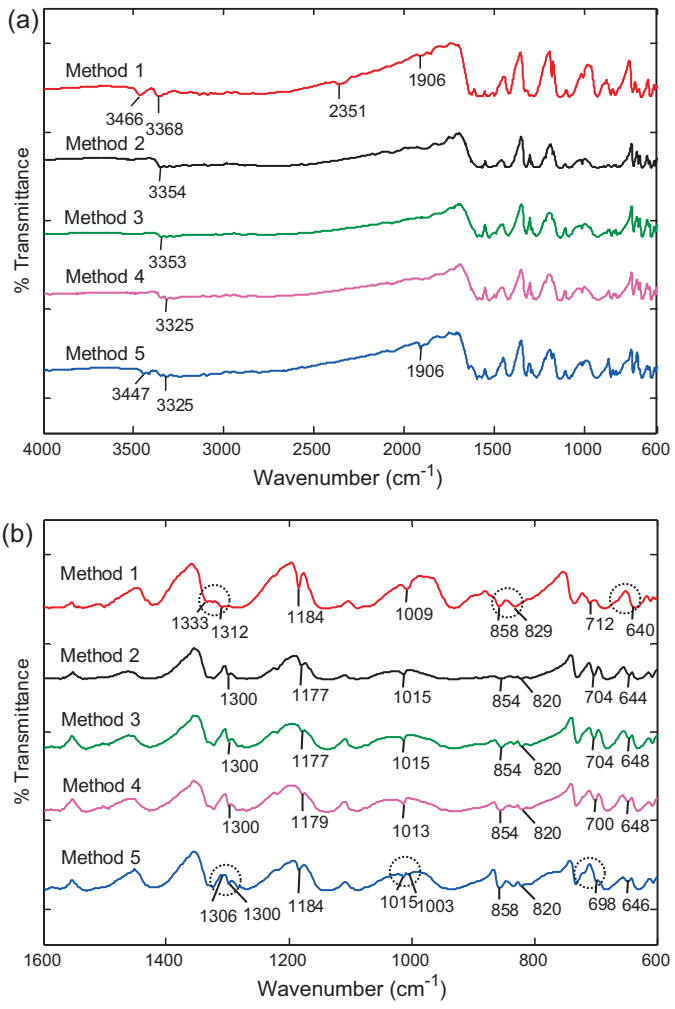

Fig. 15. FT-IR spectra of crystals obtained from Method 1, Method 2, Method 3, Method 4 and Method 5 arranged in order from top to bottom between (a) 600 and 4000 cm^{-1} and (b) 600 and 1600 cm^{-1}.

requires close examination. For this reason, the curve was re-plotted together with the TG curve and they are presented in Fig. 13. Below 200 °C, the curves can be divided into three parts according to different reactions: (A) 106–129 °C: dehydration of a hydrate species called isolated site hydrate with loosely bound water; (B) 129–153 °C: dehydration of tightly bound water from the sulfathiazole hydrate; and (C) 153–171 °C: removal of the trapped volatile impurities due to polymorphic transformation. The mole fraction of the solvent removed by the dehydration processes (A and B) is calculated to be 0.0206, while that removed by the polymorphic transformation is 0.0024. The results of the DSC, TG and HSM analyses indicate that some of the crystals obtained by Method 4 are hydrates, while some transformed to Form I at a temperature between 160.8 °C and 168.3 °C. Those few crystals that have not transformed to Form I, melted at 180.8 °C. The newly formed Form I melted at a temperature between 201.8 °C and 203.3 °C.

Results of the DSC and TG analyses of the crystals obtained by Method 5 are shown in Fig. 7(e). The DSC curve shows two endothermic peaks. The onset of the first peak is at 196.5 ± 0.1 °C, while that of the second is at 202.0 ± 0.0 °C. Two thermal events were also shown by the HSM analysis. It can be seen from a snapshot of the crystals during HSM analysis in Fig. 14(c) that all crystals, except the highlighted ones, melted at 198.2 °C. The highlighted crystals started to melt at 201.8 °C, as can be observed in Fig. 14(d). A complete melting of Form V crystals at a temperature between 196.0 °C and 196.5 °C was previously reported (Lagas and Lerk, 1981; Anwar et al., 1989), but this would only be observed if the crystals were very pure. According to Lagas and Lerk (1981), if the slightest amount of Form I was present, Form I crystallised during the melting of Form V, which was indicated by the appearance of an exothermic peak immediately after the endothermic melting peak and before the newly formed crystals melted. The presumed exothermic crystallisation peak was also observed in this work, as can be seen in Fig. 7(e). The presence of two melting peaks in this work is consistent with the work of Anderson et al. (2001). In their work, the melting peaks were observed at the onsets of 197 °C and 202 °C. In addition to the two melting peaks at the onsets of 197 °C and 201 °C, Zeitler et al. (2006) detected another endothermic peak at 156 °C. The derivative TG curve in Fig. 7(e) shows the increase in the rate of weight change started at the temperature corresponding to the onset of the first DSC melting peak, i.e. 196.5 °C. These results show that Method 5 has successfully produced crystals of Form V (that melted at 196.5 °C), but some of them have transformed to Form I undetected at some points during heating, or as suggested by Lagas and Lerk (1981) have melted and immediately recrystallised as Form I. However, there is also a possibility that Form I has formed together with Form V from the beginning; which is based on the suggestion by Lagas and Lerk (1981) that the presence of Form I may induce the recrystallisation of Form I from the melt of Form V.

5.3.3. FT-IR spectroscopy

The FT-IR spectra (600–4000 cm^{-1}) and (600–1600 cm^{-1}) of crystals obtained by all methods are presented in Fig. 15. The spectra are sufficiently distinct to characterise crystals obtained by Method 1 and Method 5 only; the others, however, are practically indistinguishable. As can be observed in Fig. 15(a), the presence of bands at 3466 and 3368 cm^{-1} is unique for the spectrum of the crystals obtained by Method 1. Although slightly shifted, the bands are consistent with the NH_2 bands in Form I that occurred at 3460 and 3355 cm^{-1}, as reported by Mesley (1971). They are also consistent with the characteristic bands for Form I crystals identified by Burger and Dialer (1983) at 3365 cm^{-1}, as well as with those identified by Anderson et al. (2001) at 3462 and 3355 cm^{-1}.

The FT-IR spectrum of the crystals obtained by Method 5, on the other hand, is found to possess distinctive bands at 3447 and 3418 cm^{-1}. They are very close to the characteristic bands for Form V crystals at 3345 and 3417 cm^{-1} as reported by Anderson

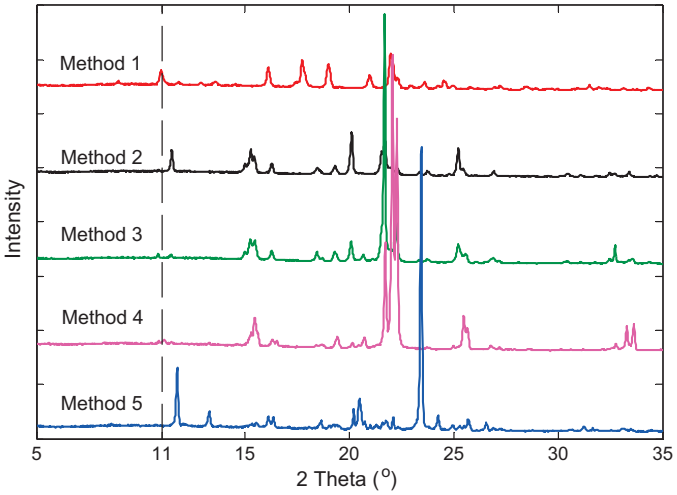

Fig. 16. XRPD patterns of crystals obtained from Method 1, Method 2, Method 3, Method 4 and Method 5 arranged in order from top to bottom. A vertical dash-line to assist in the observation for the presence of peaks at 11° 2θ.

et al. (2001). One of the bands also matched the characteristic band of Form V crystals reported by Burger and Dialer (1983) at 3445 cm^{-1}. A further examination of the FT-IR spectra in the range of 600–1600 cm^{-1}, presented in Fig. 15(b), also revealed the distinctive patterns of the spectra given by the crystals obtained by Method 1 and Method 5. As highlighted in the figure, the distinctive pattern for the crystals obtained by Method 1 are observed between 1330 and 1290 cm^{-1}, 935–820 cm^{-1} and 662–630 cm^{-1}, while those for the crystals obtained by Method 5 are detected between 1330 and 1290 cm^{-1}, 1017–965 cm^{-1} and 730–684 cm^{-1}. It has been reported in the literature that the IR spectra may not be able to distinguish clearly between sulfathiazole polymorphs (Hughes et al., 1999), particularly between Form II and Form III (Anwar et al., 1989). It was found in this work that, besides being unable to differentiate between crystals obtained by Method 2, Method 3 and Method 4, the FT-IR spectra also showed no evidence of the presence of water in the crystals obtained by Method 4. The presence of water should show interference from NH_2 absorptions near 3300 and 1650 cm^{-1} where water absorptions are expected (Mesley, 1971). The result may indicate that the presence of water in the crystals was so small that it escaped detection by the FT-IR.

5.3.4. XRPD

XRPD patterns of the crystals obtained by all five methods are shown in Fig. 16. It can be observed that each of the patterns has its own distinctive features. Although XRPD is always able to distinguish unequivocally between different polymorphs, its use in this work has some challenges. Firstly, the five polymorphs of sulfathiazole have very closely related structures, differing only in the hydrogen bonding arrangements and inter-relation between

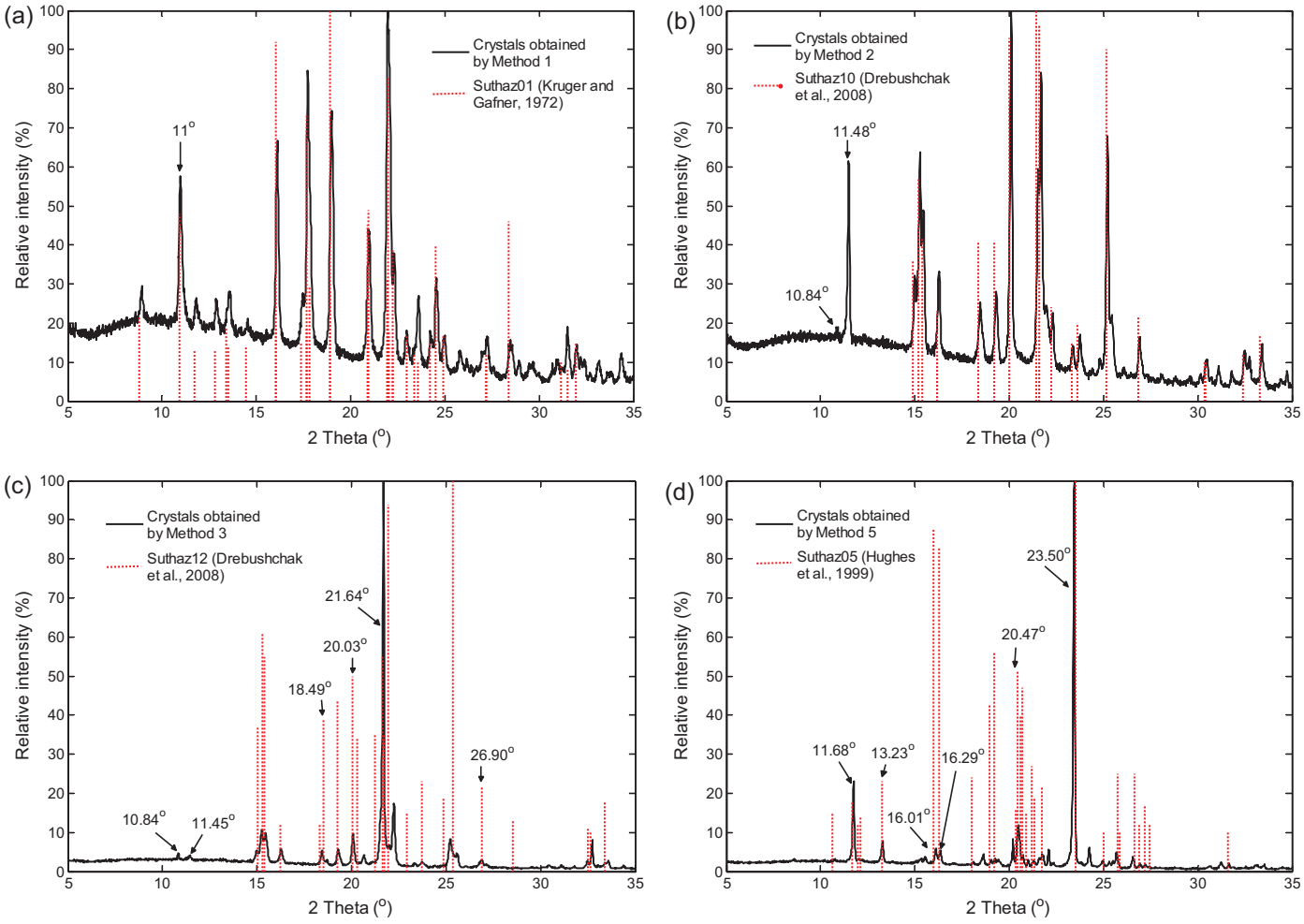

Fig. 17. XRPD patterns of crystals obtained from (a) Method 1 in comparison with some major reflections in the reference pattern of Form I (Suthaz01); (b) Method 2 in comparison with some major reflections in the reference pattern of Form II (Suthaz10); (c) Method 3 in comparison with some major reflections in the reference pattern of Form III (Suthaz12), and (d) Method 5 in comparison with some major reflections in the reference pattern (Suthaz05).

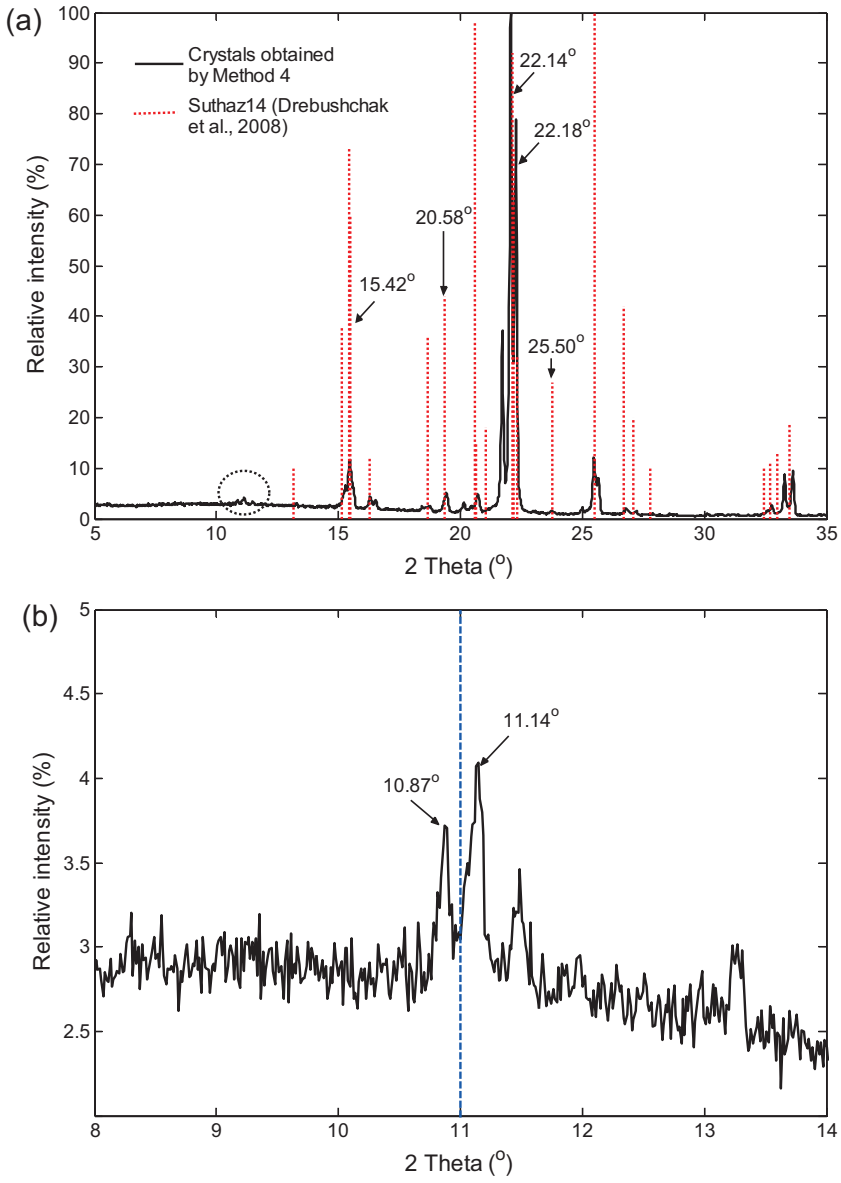

Fig. 18. (a) XRPD pattern of crystals obtained from Method 4 in comparison with some major reflections in the reference pattern (Suthaz14); and (b) zoom-out view of the circled part on the XRPD pattern in (a).

the molecules in the asymmetric unit (Blagden et al., 1998). This resulted in many of the strong reflections of each polymorph lie within the same 20–30° region, as can be seen in Fig. 16. Low angle (<20°) data, where there are fewer overlapping reflections, therefore contain the most information for distinguishing between the different polymorphs. However these may be relatively weak and hence require careful scrutiny. Secondly, there is a case called preferred orientation, which is generated when crystals line up preferentially along particular directions due to their morphology. In the case of sulfathiazole, several polymorphs exist where the crystals have plate-like or rod-like morphology. Platelets typically line up in a stacking sequence, while rods line up parallel similar to matchsticks in a box. This partially organized set-up is far from the totally random arrangement of the crystals required to observe the expected intensities of the reflections, which should be observed based on the unit cell lattice parameters and arrangement of the atoms within it. Generally the plate-like and rod-like crystals demonstrated preferred orientation along the long axis direction, which means these reflections are unexpectedly strong. However, by using the presence of the reflections, rather than their intensity, the occurrence of each polymorph can be evaluated.

Anwar et al. (1989) and Blagden (2001) have reported that the pattern of Form I can be distinguished by its characteristic peak at a 2θ value of 11°. With the assistance of a vertical dash-line, as shown in Fig. 16, it can be observed that peaks at 11° 2θ are only present on the XRPD patterns of Method 1 and Method 4. The peak on the latter pattern, however, is so tiny that it may require close examination. The patterns in Fig. 16 are individually analysed and discussed in the subsequent paragraphs.

Fig. 17(a) shows the XRPD pattern of the crystals obtained from Method 1 in comparison with some major reflections (10% relative intensity) in the XRPD data of Form I (Suthaz01) contributed by Kruger and Gafner (1972), obtainable from the CSD. It can be seen from the figure that the pattern of the crystals obtained from Method 1 concurs very well with the reference data. As previously mentioned, the characteristic peak of Form I at 11° 2θ is present on the pattern. This confirms the results of other characterisation techniques that pure Form I crystals have been successfully produced by Method 1.

Fig. 17(b) presents the XRPD pattern of the crystals obtained from Method 2 in comparison with the CSD's XRPD data of Form II (Suthaz10) contributed by Drebushchak et al. (2008). This data reference was chosen instead of the earlier one by Kruger and Gafner (1971) because of its better quality of the structure determination. Except a reflection at 11.48°, all other major reflections in the XRPD pattern of the obtained crystals concur very well with those of the reference data. The reflection at 11.48° however corresponds to a peak at 11.40° in the reference data, only that the latter relative intensity is only 2% (hence it is not shown in the figure), while the former is 61%. This extreme difference in the relative intensity may be contributed by the preferred orientation as mentioned previously. The absence of a peak at 11° 2θ on the pattern indicates the absence of Form I in the sample. Since in this case almost all peaks in the XRPD pattern of the obtained crystals agree well with the reference data, it can be confirmed that Method 2 is a reliable method of producing Form II crystals.

The comparison of the XRPD pattern of crystals obtained from Method 3 with the major reflections in the reference data for Form III (Suthaz12), supplied by Drebushchak et al. (2008) in the CSD, is presented in Fig. 17(c). In this case, the difference in intensity is very large; most reflections of the obtained crystals are much less intense compared to the reference. Extreme cases may contribute to the complete absence of a few reflections in the crystals' XRPD pattern, which are present in the reference. However, since most of the reflections present in the crystals' XRPD pattern concur very well with those of the reference, particularly at the characteristic reflections of Form III at 18.49°, 20.03°, 21.64° and 26.90°, it confirms that Method 3 has successfully produced Form III crystals. Since Form I is not present in the sample as can be inferred from the absence of the characteristic peak of Form I at 11° 2θ, the transformation of Form III to Form I crystals, as shown by the DSC and the derivative TG curves in Fig. 7(c), can proceed without any contamination of Form III with Form I.

The XRPD pattern of crystals obtained from Method 4 as depicted in Fig. 18(a) also shows that most of its reflections are less intense compared to the reference data of Form IV (Suthaz14) given by Drebushchak et al. (2008) in the CSD. There is also an absence of a few of the reflections in the crystals' XRPD pattern that are present in the reference. Form I is not present in the crystals since its characteristic peak at 11° 2θ is absent from the pattern, as can be seen from Fig. 18(b), which shows a zoom-out view of the circled part on the XRPD pattern in Fig. 18(a). The concurrence of most of the reflections in the crystals' pattern with those of the reference, particularly at the characteristic reflections of Form IV at 15.42°, 20.58°, 22.14°, 22.18° and 25.50° as shown in Fig. 18(a), proves that Method 4 is a reliable method to produce Form IV crystals.

Fig. 17(d) shows the XRPD pattern of crystals obtained from Method 5 together with the CSD's pattern of Form V (Suthaz05) contributed by Hughes et al. (1999). It was found that the pattern of the crystals under investigation shares the characteristic reflections of Form V at 11.68°, 13.23°, 16.01°, 16.29°, 20.47° and 23.50°. No peak at 11° 2θ is observed, which indicates the absence of Form I crystals. Therefore, the possibility that Form I has formed together with Form V from the beginning, as suggested earlier, can be eliminated. It can now be confirmed that Method 5 is a reliable method to produce Form V crystals.

In this work, although the normal procedure of grinding samples to a fine powder to present the crystals in a random orientation to the incident X-ray beam was followed, the results of the XRPD analysis indicates that no polymorphic transformations had occurred. This is in agreement with Anwar et al. (1989), who studied the effect of grinding of a sulfathiazole polymorph on the XRPD pattern. Besides the absence of polymorphic transformation, they also found that the XRPD pattern improved significantly with the increase in grinding.

6. Conclusions

The crystallisations of sulfathiazole polymorphs using selected literature methods were carried out with their processes monitored and recorded using FBRM and ATR-UV spectroscopy. Various solid-state characterisation techniques have been utilised to assess the success of these crystallisation processes. The results of the thermal analysis (DSC, TG and HSM), FT-IR spectroscopy and XRPD have shown that the crystals obtained from Method 1 and Method 5 are pure Form I and Form V, respectively. For the crystals obtained from Method 2, Method 3 and Method 4, the results of the thermal analysis have indicated that some of the crystals have transformed to Form I in a temperature range of 130–168 °C. Those crystals that were not transformed melted at a temperature between 173 °C and 182 °C, while the newly formed Form I crystals melted at a temperature between 201.7 °C and 203.3 °C. The results of the thermal analysis also indicate that some of the crystals obtained by Method 4 are hydrates. The FT-IR spectra of the crystals obtained by Method 2, Method 3 and Method 4 were found to be identical; therefore it is not possible to differentiate between them. The obtained XRPD patterns for the crystals obtained by Method 2, Method 3 and Method 4 matched well with the CSD patterns for Form II, Form III and Form IV, respectively. The patterns also showed the absence of Form I in the obtained crystals, which indicates the presence of Form I detected by the thermal analysis was the result of the polymorphic transformation during heating. The results show that all of the selected crystallisation methods are able to produce the desired pure polymorphs.

The *in situ* monitoring and recording of the crystallisation processes of the polymorphs allow the design range of the process parameters that has been demonstrated to produce the desired crystal quality to be defined. The process parameters in this case refer to the evolution of the temperature, FBRM total counts/s and UV absorbance. By operating within the defined design range, the crystals can be reproduced with a guaranteed quality and minimum risk. The incorporation of the process and product knowledge into the process design is part of the PAT framework and satisfies the Quality-by-Design concept (Wu et al., 2010). The ultimate aims are to reduce wastage, manufacturing error, time to market and costs of drugs. In the context of the present work, it is hoped that the availability of the defined design range of the process parameters will contribute towards the availability of clear and adequate description of the crystallisation conditions that are able to consistently produce the intended pure sulfathiazole polymorph.

Acknowledgements

The authors thank Dr. David Ross for the HSM system and Frank Page for the SEM imaging – all were carried out in the Department of Materials, Loughborough University. Financial support provided by the Engineering and Physical Sciences Research Council (EPSRC), U.K. (grant EP/E022294/1) is also gratefully acknowledged. The first author is grateful to the Malaysian Ministry of Higher Education for a scholarship.

Appendix A.

See Fig. A.1.

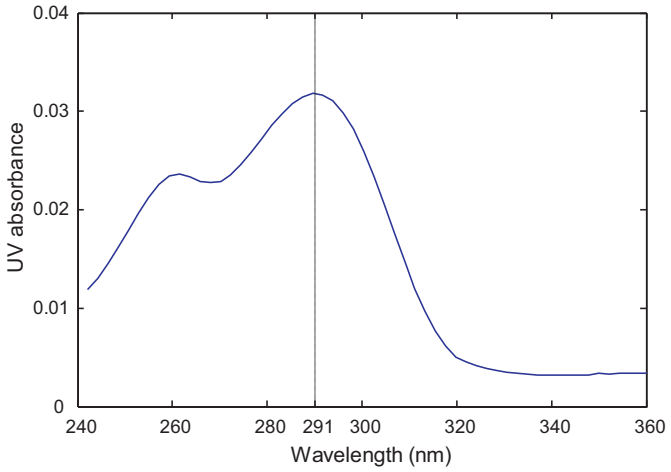

Fig. A.1. Typical absorbance spectra of sulfathiazole in *sec*-butanol saturated at 80 °C.

References

Aaltonen, J., Rantanen, J., Siiriä, S., Karjalainen, M., Jrgensen, A., Laitinen, N., Savolainen, M., Seitavuopio, P., Louhi-Kultanen, M., Yliruus, J., 2003. Polymorph screening using near-infrared spectroscopy. Anal. Chem. 75, 5267–5273.

Abu Bakar, M.R., Nagy, Z.K., Rielly, C.D., 2009. Seeded batch cooling crystallization with temperature cycling for the control of size uniformity and polymorphic purity of sulfathiazole crystals. Org. Process Res. Dev. 13, 1343–1356.

Ali, H.R.H., Edwards, G.M., Scowen, I.J., 2009. Insight into thermally induced solid-state polymorphic transformation of sulfathiazole using simultaneous in situ Raman spectroscopy and differential scanning calorimetry. J. Raman Spectrosc. 40, 887–892.

Alvarez, A.J., Singh, A., Myerson, A.S., 2009. Polymorph screening: comparing a semi-automated approach with a high throughput method. Cryst. Growth Des. 9, 4181–4188.

Anderson, J.E., Moore, S., Tarczynski, F., Walker, D., 2001. Determination of the onset of crystallization of N1-2-(thiazolyl)sulfanilamide (sulfathiazole) by UV–vis and calorimetry using an automated reaction platform; subsequent characterization of polymorphic forms using dispersive Raman spectroscopy. Spectrochim. Acta A 57, 1793–1808.

Anwar, J., Tarling, S.E., Barnes, P., 1989. Polymorphism of sulphathiazole. J. Pharm. Sci. 78, 337–342.

Apperley, D.C., Fletton, R.A., Harris, R.K., Lancaster, R.W., Tavener, S., Threlfall, T.L., 1999. Sulfathiazole polymorphism studied by magic-angle spinning NMR. J. Pharm. Sci. 88, 1275–1280.

Babilev, F.V., Belskii, V.K., Simonov, Y.A., Arzamastev, A.P., 1987. Polymorphism of norsulphazol. Khim.-Farm. Zh. 21, 1275–1280.

Bernstein, J., 2002. Polymorphism in Molecular Crystals. Clarendon Press, Oxford.

Billot, P., Couty, M., Hosek, P., 2010. Application of ATR-UV spectroscopy for monitoring the crystallization of UV absorbing and non-absorbing molecules. Org. Process Res. Dev. 14, 511–523.

Bingham, A.L., Hughes, D.S., Hursthouse, M.B., Lancaster, R.W., Tavener, S., Threlfall, T.L., 2001. Over one hundred solvates of sulfathiazole. Chem. Commun. 7, 603–604.

Blagden, N., 2001. Crystal engineering of polymorph appearance: the case of sulphathiazole. Powder Technol. 121, 46–52.

Blagden, N., Davey, R.J., Lieberman, H.F., Williams, L., Payne, R., Roberts, R., Rowe, R., Docherty, R., 1998. Crystal chemistry and solvent effects in polymorphic systems: sulfathiazole. J. Chem. Soc., Faraday Trans. 94, 1035–1044.

Burger, A., Dialer, R.D., 1983. Neu untersuchungsergebnisse zur polymorphie von sulfathiazole. Pharm. Acta Helv. 58, 72–78.

Carless, J.E., Jordan, D., 1974. The dissolution kinetics of sulfathiazole Form I. J. Pharm. Pharmacol. 26, 86P–87P.

Chan, F.C., Anwar, J., Cernik, R., Barnes, P., Wilson, R.M., 1999. Ab initio structure determination of sulfathiazole polymorph V from synchrotron X-ray powder diffraction data. J. Appl. Crystallogr. 32, 436–441.

Drebushchak, T.N., Boldyreva, E.V., Mikhailenko, M.A., 2008. Crystal structures of sulfathiazole polymorphs in the temperature range 100–295 K: a comparative analysis. Zh. Strukt. Khim. 49, 84–94.

Fosbinder, R.J., Walter, L.A., 1939. Sulfanilamido derivatives of heterocyclic amines. J. Am. Chem. Soc. 61, 2032–2033.

Gelbrich, T., Hughes, D.S., Hursthouse, M.B., Threlfall, T.L., 2008. Packing similarity in polymorphs of sulfathiazole. CrystEngComm 10, 1328–1334.

Gillon, A.L., Steele, G., Nagy, Z.K., Makwana, N., Rielly, C.D., 2006. PAT investigations into the crystallization of caffeine. In: 13th International Workshop on Industrial Crystallization (BIWIC 2006) , Delft, The Netherlands.

Grove, D.C., Keenan, G.L., 1941. The dimorphism of sulfathiazole. J. Am. Chem. Soc. 63, 97–99.

Guillory, J.K., 1967. Heats of transition of methylprednisolone and sulfathiazole by a differential thermal analysis method. J. Pharm. Sci. 56, 72–76.

Hakkinen, A., Pollanen, K., Karjalainen, M., Rantanen, J., Loui-Kultanen, M., Nystrom, L., 2005. Batch cooling crystallization and pressure filtration of sulfathiazole: the influence of solvent composition. Biotechnol. Appl. Biochem. 41, 17–28.

Higuchi, W.I., Bernardo, P.D., Mehta, S.C., 1967. Polymorphism and drug availability. II. Dissolution rate behavior of the polymorphic forms of sulfathiazole and methylprednisolone. J. Pharm. Sci. 56, 200–207.

Howard, K.S., Nagy, Z.K., Saha, B., Roberston, A.L., Steele, G., Martin, D., 2009. A process analytical technology based investigation of the polymorphic transformations during the antisolvent crystallization of sodium benzoate from IPA/water mixture. Cryst. Growth Des. 9, 3964–3975.

Hughes, D.S., Hursthouse, M.B., Threlfall, T., Tavener, S., 1999. A new polymorph of sulfathiazole. Acta Crystallogr. C 55, 1831–1833.

Jordan, D., Carless, J.E., 1976. The crystallization behaviour of sulfathiazole. J. Pharm. Pharmacol. 28, 410–414.

Karjalainen, M., Airaksinen, S., Rantanen, J., Aaltonen, J., Yliruusi, J., 2005. Characterization of polymorphic solid-state changes using variable temperature X-ray powder diffraction. J. Pharm. Biomed. Anal. 39, 27–32.

Khoshkhoo, S., Anwar, J., 1993. Crystallization of polymorphs: the effect of solvent. J. Phys. D: Appl. Phys. 26, 890–893.

Kruger, G.J., Gafner, G., 1971. The crystal structure of sulfathiazole II. Acta Crystallogr. B 27, 326–333.

Kruger, G.J., Gafner, G., 1972. The crystal structures of polymorphs I and II of sulphathiazole. Acta Crystallogr. B 28, 272–283.

Kuhnert-Brandstätter, M., Wunsch, S., 1969. Polymorphism and mixed crystal formation in sulfonamides and related compounds. Mikrochim. Acta 6, 1297–1307.

Lagas, M., Lerk, C.F., 1981. The polymorphism of sulphathiazole. Int. J. Pharm. 8, 25–33.

Lott, W.A., Bergeim, F.H., 1939. 2-(p-Aminobenzenesulfonamido)-thiazole: a new chemotherapeutic agent. J. Am. Chem. Soc. 61, 3593–3594.

Luner, P.E., Majuru, S., Seyer, J.J., Kemper, M.S., 2000. Quantifying crystalline form composition in binary powder mixtures using near-infrared reflectance spectroscopy. Pharm. Dev. Technol. 5, 231–246.

McCrone, W.C., 1965. Polymorphism. In: Fox, D., Labes, M.M., Weissberger, A. (Eds.), Physics and Chemistry of the Organic Solid State, vol. 2. John Wiley & Sons Inc., New York, pp. 725–767.

Mesley, R., 1971. The polymorphism of sulfathiazole. J. Pharm. Pharmacol. 23, 687–694.

Mesley, R.J., Houghton, E.E., 1967. Infrared identification of pharmaceutically important sulfonamides with particular reference to the occurrence of polymorphism. J. Pharm. Pharmacol. 19, 295–304.

Miller, R.P., Sommer, G., 1966. A hot stage microscope incorporating a differential thermal analysis unit. J. Sci. Instrum. 43, 293–297.

Milosovich, G.J., 1964. Determination of solubility of a metastable polymorph. Pharm. Sci. 53, 484–487.

Miyazaki, H., 1947. Polymorphism and melting points of sulfathiazoles. Jpn. J. Pharm. Chem. 19, 133–134.

Moustafa, M.A., Carless, J.E., 1969. Application of differential scanning calorimetry to the study of sulfathiazole crystal forms. J. Pharm. Pharmacol. 21, 359–365.

Myerson, A.S., 2002. Handbook of Industrial Crystallization. Butterworth-Heinemann Ltd., Oxford.

Nagy, Z.K., Gillon, A.L., Steele, G., Makwana, N., Rielly, C.D., 2007. Using process analytical technology for in situ monitoring of the polymorphic transformation of organic compounds. In: Proceedings of the 8th International Symposium on Dynamics and Control of Process Systems (DYCOPS). 3. Foss B, Alvarez J. IFAC , Cancum, Mexico, pp. 133–138.

Parmar, M.M., Khan, O., Seton, L., Ford, J.L., 2007. Polymorph selection with morphology control using solvents. Cryst. Growth Des. 7, 1635–1642.

Pollanen, K., Hakkinen, A., Huhtanen, M., Reinikainen, S.-P., Karjalainen, M., Rantanen, J., Louhi-Kultanen, M., Nystrom, L., 2005. Drift-IR for quantitative characterization of polymorpic composition of sulfathiazole. Anal. Chim. Acta 544, 108–117.

Shaktshneider, T.P., Boldyrev, V.V., 1993. Phase transformations in sulfathiazole during mechanical activation. Drug Dev. Int. Pharm. 19, 2055–2067.

Shami, E.G., Bernardo, P.D., Rattie, E.S., Ravin, L.J., 1972. Kinetics of polymorphic transformation of sulfathiazole Form I. J. Pharm. Sci. 61, 1318–1320.

Shenouda, L.S., 1970. Various species of sulfathiazole Form I. J. Pharm. Sci. 59, 785–787.

Simon, L.L., Nagy, Z.K., Hungerbuehler, K., 2009. Comparison of external bulk video imaging with focused beam reflectance measurement and ultra-violet visible spectroscopy for metastable zone identification in food and pharmaceutical crystallization processes. Chem. Eng. Sci. 64, 3344–3351.

Warrington, S.B., 2002. Simultaneous thermal analysis techniques. In: Haines, P.J. (Ed.), Principles of thermal analysis and calorimetry, Cambridge: The Royal Society of Chemistry, pp. 166–189.

Wu, H., White, M., Khan, M.A., 2010. Quality-by-Design (QbD): an integrated process analytical technology (PAT) approach for a dynamic pharmaceutical co-precipitation process characterization and process design space development. Int. J. Pharm., doi:10.1016/j.ijpharm.2010.11.045.

Yu, L.X., Lionbergera, R.A., Rawa, A.S., D'Costa, R., Wub, H., Hussain, A.S., 2003. Applications of process analytical technology to crystallization processes. Adv. Drug Delivery Rev. 56, 349–369.

Zeitler, J.A., Newnham, D.A., Taday, P.F., Threlfall, T.L., Lancaster, R.W., Berg, R.W., Strachan, C.J., Pepper, M., Gordon, K.C., Rades, T., 2006. Characterization of temperature-induced phase transitions in five polymorphic forms of sulfathiazole by terahertz pulsed spectroscopy and differential scanning calorimetry. J. Pharm. Sci. 95, 2486–2498.